INVESTIGATION OF SEDIMENT PATHWAYS IN HIDDEN RIVER CAVE, KENTUCKY

INVESTIGATION OF SEDIMENT PATHWAYS IN HIDDEN RIVER CAVE, KENTUCKY

By SAMANTHA KATHERINE FEIST, B.Sc.

A Thesis Submitted to the School of Graduate Studies in Partial Fulfilment of the Requirements for the Degree Master of Science

McMaster University MASTER OF SCIENCE (2017) Hamilton, Ontario (Earth and Environmental Science)

TITLE: Investigation of sediment pathways in Hidden River Cave, Kentucky

AUTHOR: Samantha K. Feist, B.Sc. (University of Guelph)

SUPERVISORS: Professor J.C. Maclachlan and Professor C.H. Eyles

NUMBER OF PAGES: xii, 69

Abstract

Karstic cave systems are intricately related to surficial processes and the study of cave sediments is a growing field of research. Sediment deposits in caves are protected from surficial weathering processes, and are therefore often preserved. Cave sediments have applications in studies for paleoclimatic reconstruction, contaminant transport, and paleoflood and stream incision rates, making them valuable contributors to other areas of geoscience. Hidden River Cave is an active, multi-level cave system in the town of Horse Cave, Kentucky with over 33 km of mapped passages. A history of anthropogenic impacts on the cave system include uses for hydroelectric power generation, a water source, and a show cave until it closed in 1943 due to severe contamination from domestic and industrial waste. This study reports on the analysis of sediment cores collected from the cave system which show distinct concentrations of metals within the sediment from chrome plating plant effluent. Relative concentrations of metals in the core record were obtained using an ITRAX core scanner, and were observed to decrease moving downstream from the chrome plating plant contamination source. Sediment core analysis allows depositional patterns in the cave system to be observed and related to historic surficial processes. The chronology of sedimentation events was determined using Pb-210 analysis of core sediment and indicates a strong connection between historical contaminating events in the town of Horse Cave and cave sediment deposition. Sediment core analysis has thus allowed depositional patterns in the cave system to be determined and related to historic surficial processes. These findings can be applied to enhance understanding of the combined effects of landscape evolution and anthropogenic

impacts which may be used to inform decision making processes for communities overlying both Hidden River Cave and other karstic cave systems.

Acknowledgements

Appreciation for funding for this thesis project goes to the School of Geography and Earth Sciences at McMaster University through the Walker-Middleton award, the American Cave Museum and Hidden River Cave via the Kentucky Division of Water, Source Waters Protection Assistance Program, and the Cave Research Foundation.

I would like to thank my supervisors Dr. John Maclachlan and Dr. Carolyn Eyles for all their guidance and assistance through the past two years. The time they have spent helping, and their unwavering confidence in my abilities is greatly appreciated and invaluable. I can truly say I feel I have learned and grown so much over the past two years and am so thankful for the opportunity I have had to work with John and Carolyn. I would also like to thank Dr. Eduard Reinhardt for his advice, guidance and lab space at various times through this project, and to Russ Ellis and the integrated science lab for graciously allowing us space for lab work.

This work would not have been possible without the American Cave Museum/American Cave Conservation Authority, and their continued support and excitement about our partnership. Thank you to Dave Foster, whose support for this research and willingness to welcome us back to Hidden River again and again is greatly appreciated; to Peggy Nims, our unwavering and fearless cave guide who was integral to this research; and to all the other staff at the American Cave Museum for always welcoming us back to the cave. A thank you also to Tom Chaney, who graciously spent many hours telling us about the

history of Horse Cave, and to Virginia Davis at the Hart County Chamber of Commerce. Thank you to Rick Olson for feedback and spectacular tours in Mammoth Cave, and to those from Western Kentucky University who provided insight and expertise that greatly assisted the research and methodologies.

Thank you to all of those who have been a part of the field trips to Kentucky the past two years, for their fearless trekking through the cave and willingness to let Hidden River challenge them: Rebecca Lee, Lauren Oldfield, Jason Brodeur, Spencer Williams, Chelsi McNeill-Jewer, Anya Krywy-Janzen, Mitchell Davidson, Katie Maloney and Winnie Chan. A thank you also to all those in the Glacial Lab including Rodrigo Narro-Perez, Riley Mulligan and Logan Jung-Ritchie.

And finally, thank you to my mom and dad, and to my sisters Alison and Rachel for all their support through these past two years. Thank you to Corey Goad, for helping to keep me sane for what has probably been the craziest summer of my life; for being a sounding board and for just simply being there for support during the writing process. And thank you my friends Cameron Curran, Ali Gamble, Maddy Jones, Garrett Patriquin and those unlisted for their support.

I am immensely grateful to all those listed and unlisted that aided in the completion of this research throughout the entire process.

Table of Contents

List of Figures

List of Tables

1. Introduction and Background

Cave science, which consists of either applied research (e.g. resolution of land use problems stemming from subsurface cave formation) or basic research (e.g. data collection from within the cave system for enhancing understanding of cave formation) in general is considered by many to be an "immature" field of science (Mylroie & Sasowsky; 2004). While cave sediments have always been acknowledged as an integral part of cave systems, their importance to scientific research has only been appreciated in the past few decades (White, 2007). Cave sedimentology is an expanding field of research, with applications in geology, hydrogeology, paleoclimate studies, archaeology, evolutionary biology, geomicrobiology, and mineralogy (Springer et al., 1997; Dogwiler & Wicks, 2004; Kambesis, 2007; White, 2007; Farrant & Smart, 2011). Specific applications of cave sedimentology include paleoclimatic reconstructions (White, 2007; Hauselmann, 2008), the understanding of contaminant transport (Mahler et al., 1999; Herman et al., 2012) and establishing paleoflood and stream incision rates (Springer et al., 1997; White, 2007; Plotnick et al., 2009). These applications offer unique opportunities to use cave deposits to explore past geomorphic processes and their relationship to the development of cave systems. The sediment type and its characteristics can be used to identify where the sediment came from, and its processes of transport and deposition.

Caves are considered to be an important element of karst environments. These environments are identified by their morphological and hydrological characteristics, which are formed by dissolution of soluble rocks, commonly carbonates and evaporites

(Ford & Williams, 2007; De Waele et al., 2009). Karst landscapes make up approximately 10% of the Earth's surface, and karst aquifers supply approximately 25% of drinking water in global populations (U.S. Department of the Interior, 2014). Karst forms as surface water penetrates cracks in soluble rocks, enlarging the cracks by dissolution forming conduits, and eventually larger voids and subsurface cave passages. Cave systems are therefore intricately linked to surficial processes and the behaviour of both surface water and groundwater. Surface water can rapidly enter the subsurface karst system making karst environments particularly susceptible to contamination from anthropogenic sources as there is little time for potential contaminants to be filtered out or to decompose through natural processes (Mahler et al., 1999; Ford & Williams, 2007). This is a concern for communities that rely on potable water from karstic sources and emphasizes the importance of protecting and monitoring the quality of groundwater in such areas (Mahler et al., 1999). Few studies of cave sediments have established a clear connection between episodes of known contaminant release and changes in the composition of cave sediments, although such correlations have been made using lake sediments (Miller et al., 2015; Lintern et al., 2016). Many anthropogenic contaminants, including chromium, nickel and copper, adsorb onto sediment, and require an understanding of how sediment is both transported and deposited to allow predictions of potential contaminant distribution.

This study examines the physical and chemical characteristics of sediments accumulating in the Hidden River Cave system in Kentucky (Figure 1). This cave system underlies the town of Horse Cave and has been severely impacted by industrial

contamination during the past 50 years. The aim of the study is to integrate evidence from multiple sources including historic land use practices, sedimentology (sediment chronology and elemental analysis), and field-based observations to enhance understanding of sediment dynamics and the transport and accumulation of contaminants in a cave system.

1.1 Karst Landscape Evolution and Cave Development

Hidden River Cave in Kentucky underlies the town of Horse Cave (Figure 1) and is hydrogeologically related to Mammoth Cave, the longest cave system in the world (Kambesis, 2007). Mammoth Cave is located 17 km northwest of Horse Cave in Mammoth Cave National Park (Figure 1). The Mammoth Cave system is geomorphically more developed than Hidden River Cave, and can be used to help understand the processes of evolution occurring in Hidden River Cave, which is a relatively young cave system. The Hidden River Cave system is carved out of Mississippian limestone deposits, which underlie much of the surrounding region (Pohl, 1970; White et al., 1970; Blair et al., 2012).

Cave systems form elements of karst landscapes that evolve over time through the weathering and dissolution of carbonate rocks. It is thought that karst landscapes evolve following three general stages of physiographic evolution (White et al., 1970). The first stage is pre-karst high-relief topography, where there are thick capping beds, such as chert, sandstone or shale, above the carbonate rock. At this point, few streams have infiltrated the carbonate unit due to the overlaying cap rock, and there is little

development of sinkholes and other karst features. As rivers continue to slowly cut into the cap rock, the system enters the second stage, displaying precursors to karst development. By this stage rivers have cut into the cap rock creating narrow, steep-walled valleys and drainage is diverted underground, forming and widening fractures in the rock. As the cap rock is removed over time these dissolutional effects are compounded, leading to the third stage of karst development, an environment with extensive karst terrain including karst valleys, subsurface karst features, and sinkholes. Cave passage development is a result of continued dissolution and conduit widening (White & White, 1968). The transfer from a fluvial-dominated to karst-dominated landscape is dependent on how well subsurface drainage can continually evolve and increase in its capacity to support fluid flow (Groves & Meiman, 2005). Systems that can transmit more flow experience more flow diversion underground, resulting in less surface drainage and increased surficial expression of karst features such as sinkhole plains (Groves & Meiman, 2005). Portions of the Mammoth Cave system may have developed in this way.

As karst development continues, rivers continue to erode within the cave system and base level lowers, eventually to the point that entire flow paths are abandoned as the predominant stream flow moves downward (Bosch & White, 2004). Abandoned passages may experience water flow during large flood events until the stream level decreases to the point where water no longer reaches upper cave levels, so sediment deposits in these abandoned passages will not experience further reworking and the sediment record, including the final depositional event, will be preserved (Bosch & White, 2004).

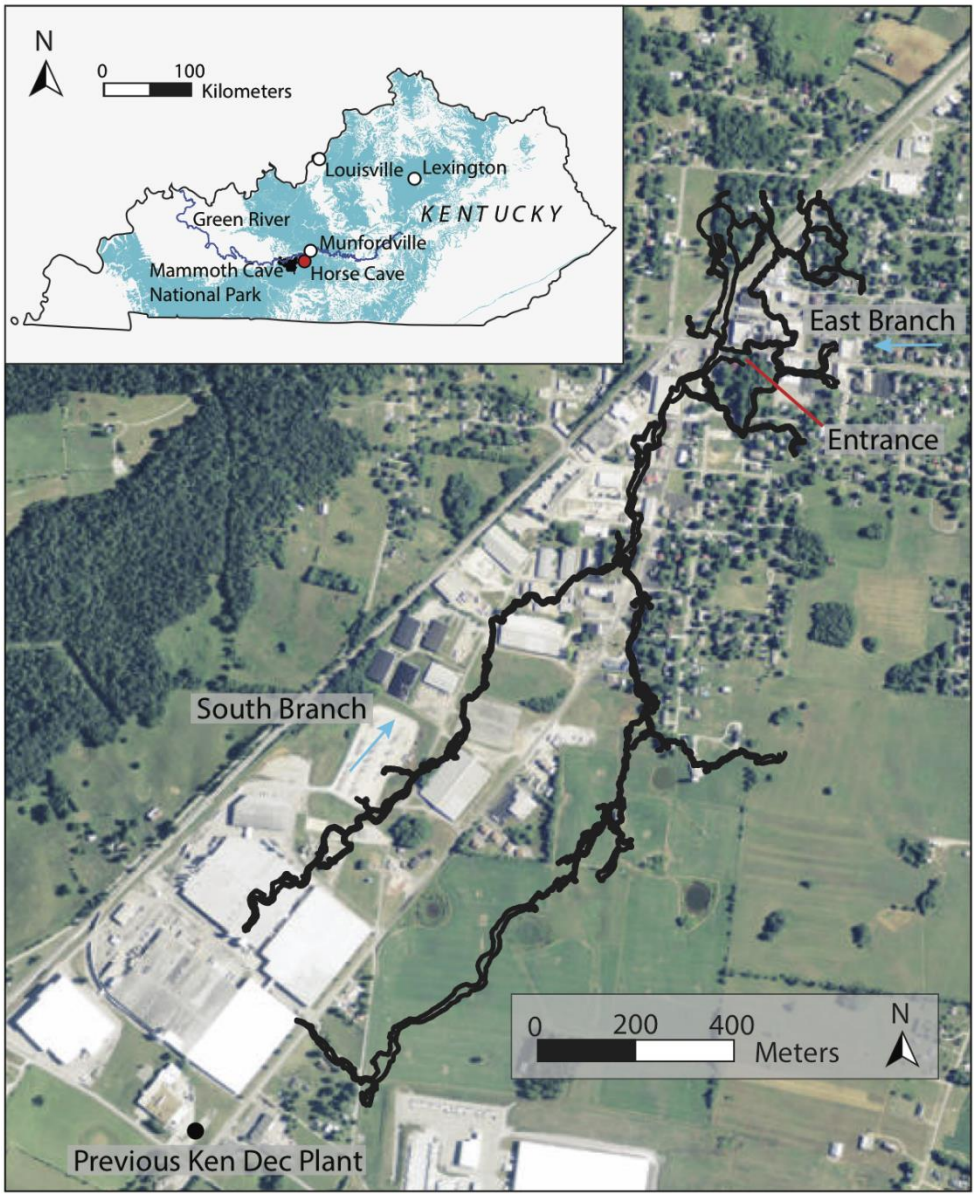

Figure 1: Study Site Map. The map of the Hidden River Cave passages (in black) overlain on satellite imagery of the Horse Cave area. The red line points to the entrance to the cave system in downtown Horse Cave. The cave system extends further northeast than the extent of this figure. Water flow in the cave system moves in a northeast direction. Note the industrial area in the southwest corner of the map, with the location of the previous Ken Dec chrome plating plant labelled. The inset shows the State of Kentucky, with major cities (Louisville and Lexington), the nearby Mammoth Cave National Park (shaded in black), and the Green River for reference. The town of Horse Cave is shown with a red marker. Blue shading indicates areas with bedrock that have potential for karst development. (*Cave passages map modified from Dave West, 2013; Satellite imagery from bernszukalski, ArcGIS.com; Esri; Inset modified from Google Earth, 2017 using USGS (2017), US Department of the Interior: NPS (2004), & Paylor & Currens (2001) (via KGS & UKy, 2010)).*

Sediment deposits in caves have been found to record events from as early as the late Pliocene to the present (Bosch & White, 2004). The Mammoth Cave system in Kentucky contains multiple levels of cave passages, and is dry on upper levels with active streams on lower levels. Mammoth Cave is a good example of the effects of downward stream incision which has left several upper level passages dry and no longer experiencing water flow or sediment reworking. The Hidden River Cave system is not as well developed as Mammoth Cave and has an active stream affecting two levels, with upper levels still experiencing periodic flow from flood events.

Water chemistry and flow data have been analysed in the Cave City, Kentucky groundwater basin to quantify landscape denudation processes in the basin, processes which impact the evolution of karst passages and determine whether drainage will be on the surface, in the subsurface, or a combination of both (Groves and Meiman, 2005). Their results can be applied to help deduce whether primarily karst or fluvial processes are shaping the surficial landscape characteristics (Groves & Meiman, 2005). Cave systems have different geometries and characteristics based on their mode of formation by either surficial water (epigenic caves) or groundwater (hypogenic caves) (Loucks, 1999). It is very apparent that caves are dynamic elements of the karst system, and reflect the combined influences of the local and regional geology, mineralogy, and hydrogeology (White et al., 1970).

1.2 Sediment Transport in Caves

1.2.1 Karst Hydrology

Hydrologically, karst systems are highly hetereogeneous and anisotropic (Ford & Williams, 2007). Limestone bedrock dissolution creates opportunities for many conduits and voids to form, creating a complex flow system. To understand sediment movement through such a system, it is crucial to understand the hydrology of the system. In surficial water basins, sediment transport and deposition is a central issue, especially in flood flows (Simon et al., 2004; Herman et al., 2012). However, in subsurface aquifers (i.e. porous media with groundwater flow) sediment transport, aside from dissolved load, is not a central focus (Herman et al., 2012). Hydrological studies of surface systems focus on the drainage basin, its drainage boundaries, study site topography, and stream channel layout within that basin. Surficial hydrological models, commonly depict water flow using stream hydrographs, and examine inputs through precipitation and storm event frequency (Herman et al., 2012).

In contrast, groundwater hydrology focuses on the aquifer strata lithology and thickness, as well as hydraulic conductivities of the aquifer material (Ford & Williams, 2007; Herman et al., 2012). Where surficial drainage basins are delineated by size, aquifer size is only delineated in terms of spatial extent of the water-bearing formations (Herman et al., 2012). Aquifers are expected to show much lower groundwater flow velocities in comparison to relatively rapid surficial flows (Herman et al., 2012). The behaviour of groundwater is influenced by the potentiometric surface (the water level in the subsurface based on hydraulic head), and Darcy's law (descriptor of flow through

porous media) which accounts for hydraulic conductivity, the ability of water to flow through a material (Freeze & Cherry, 1979; Herman et al., 2012).

Water flow through karst systems combines the flow characteristics of both surface and groundwater as the nature of karst systems involves dissolution of channels in the bedrock and general aquifer flow characteristics cannot generally be applied to these flows (Herman et al., 2012). The passage of subsurface water through tortuous and lengthy conduits in the rock results in lower flow velocities than would be experienced by surface flows (White & White, 1968). However, the movement of subsurface water is much more rapid in karst systems than in most other subsurface aquifers due to its ability to flow relatively quickly through cracks and open conduits (Herman et al., 2012). The flow characteristics of subsurface water in karst systems has critical influence on both sediment transport and deposition in cave systems (Herman et al., 2012).

1.2.2 Karst Hydrology and Sediment Transport

The variety of depositional environments and passage sizes in caves affect how sediment and water move in different areas of the cave, resulting in complex hydrology and non-homogenous deposition of sedimentary fill within the cave system (Arriolabengoa et al., 2015). The transfer of water from the surface to the subsurface, within conduits entering the karst system, allows floodwaters to rise very quickly and to rapidly entrain and transport sediment. Sediment transport in a cave system is highly episodic, with the majority of material moved during larger magnitude, intermittent high-flow flood events (Newson, 1971; Bosch & White, 2004; Plotnick et al., 2009). Karst

systems with flashy hydrographs are therefore the most effective at transporting clastic sediment, and in some instances, storm flows are higher in discharge by a factor of 100 over base flows (Bosch & White, 2004). However, sediment transport also depends on the development of the conduit system and recharge in the drainage basin (Bosch and White, 2004). This drainage capacity will depend on how quickly dissolution is occurring in the limestone bedrock (Groves & Meiman, 2005).

Understanding movement of sediment through the cave system is important for determining where and how it is deposited. There is a large variation in sediment accumulation rates in cave systems, depending upon factors such as local geological conditions and hydraulic characteristics. In phreatic or flooded caves at pipefull flow (i.e. passages are completely full of water) there is high energy for transporting sediment, and larger gravel or even boulders (if available) can be entrained (Ford & Williams, 2007). In cave passages where there is open flow or low pipefull velocities there is significantly less energy for sediment transport, and coarse sediment such as gravel and boulders will move as bedload by rolling or sliding, or not at all (Ford & Williams, 2007).

Since most cave sediment transport occurs during flood flows, it is important to understand how sediment is deposited as floodwaters wane. Fine-grained sediment is primarily deposited as slackwater facies, settling out when there is ponding water or as floodwaters wane (Ford & Williams, 2007; White, 2007). Fine-grained sediment is usually deposited parallel to the depositional surface, and individual laminae can be interpreted to be the result of rhythmic pulsing of sediment-laden water through the system (Bull, 1981; Plotnick et al., 2009). Banks of fine-grained deposits can often be

found in cave passages, building up large mounds of sediment over 20 m high in some cases and containing a fairly continuous sedimentary record (Ford & Williams, 2007). As floodwaters wane, energy levels decrease and the sides of passages are the first to experience this decrease in energy. As a result, sediment that is entrained in the flow is deposited initially at the sides of the passage near the walls, building up banks of fine-grained sediment (Gillieson, 1986; Ford & Williams, 2007). Frequent flooding and draining of passages can results in steep (> 40°) silt and clay banks, which may exhibit small stream cuts (rills) as water drains down their slopes (Ford & Williams, 2007). Banks of fine sediment such as these provide good sites for sediment analysis as they provide a high-resolution record of sedimentation events and are particularly suitable for dating sediment using isotopic techniques such as Pb-210 (Karamanos et al., 1976).

1.2.3 Sediment Transport and Contaminants

Sediment transport processes within the cave system can be used to understand how potential contaminants may move through the system and other connected groundwater resources. Metal contaminants, including chromium, nickel, and copper, sorb onto fine-grained sediment and are then deposited out of suspension with sediment particles, leaving contaminated sediment deposits in the cave system (McLean & Bledsoe, 1992; Mahler et al., 1999; Bradl, 2004). As most sediment in a cave system is moved during larger magnitude, episodic flood events (Newson, 1971; Bosch & White, 2004; Plotnick et al., 2009), any contaminants that enter the system or are already in the system will also be moved during these high-flow events. Contaminants may therefore be

deposited in sediments trapped in upper levels of the cave system during large flood events, and then later re-suspended during a subsequent flood, effectively re-distributing the contaminants.

1.3 Cave Sediment

Cave environments and their sediment deposits are protected from many surficial weathering processes. Whereas surficial landforms erode and deteriorate, cave sediments are protected from these processes such that weathering processes are relatively slow and deposits are preserved, other than being subject to disturbance by fluvial erosion processes (Sasowsky and Mylroie, 2007; Gazquez et al., 2014). Caves act as sediment traps, preserving sediment (Schroeder & Ford, 1983; Valen et al., 1997, Farrant et al., 2014, Gazquez et al., 2014) on timescales as large as 10^6 years in glacially-influenced basins (Farrant et al., 2014). Thus, evidence of geologic processes, including evolution of karstic systems, geomorphological processes, and climatic trends not preserved at the surface, may be present in cave deposits (Farrant et al., 2014).

Sediments deposited in the cave system are of two types: clastic sediment and chemical deposits (Schroeder & Ford, 1983; White, 2007; Herman et al., 2012). Clastic sediment consists of clay- to boulder-sized fragments, and is further subdivided into autogenic and allogenic material based on provenance (White, 2007; Herman et al., 2012). Autogenic material is sourced from within the cave itself, including from the breakdown of limestone rock walls; the weathering of detritus consisting of limestone, clay, sand, silicified fossil fragments, chert nodules, shale interbeds, and other insoluble

debris; and the slower accumulation of organic debris including guano (bat fecal matter; White, 2007; Herman et al., 2012). Allogenic materials are sourced from outside the cave system and enter through sinking streams in the form of alluvial material, glacial tills, volcanic ash, or any other material that can be entrained by the stream (White, 2007; Herman et al., 2012). Additionally, there is often talus buildup at cave entrances, which includes weathered bedrock and materials moved downslope from above, including soil and plant material (White, 2007).

Chemical deposits that occur within cave systems are precipitated from solution and include carbonates, evaporites, iron and manganese hydrates, ice, and phosphates (White, 2007; Herman et al., 2012). Travertine deposits are the most common on cave walls, and are precipitated carbonate deposits usually in the form of calcite or aragonite (White, 2007).

1.3.1 Sediment Facies

Sedimentary facies are not as well defined for cave systems as they are for surficial sediment deposits. Cave sediment facies are grouped according to particle size and degree of sorting, and include fluvial channel facies, thalweg facies, and slackwater facies (Springer & Kite, 1997; Bosch & White, 2004; White, 2007; Plotnick et al., 2009). Bosch and White (2004) add diamicton and backswamp facies to this assemblage (Table 1).

Table 1: Summary of sediment facies found in cave systems. Sources: Bosch & White, 2004; Ford & Williams, 2007; Plotnick et al., 2009; Springer & Kite, 1997; White 2007.

Facies	**Grain Size**	**Deposit Characteristics**	**Depositional Environment**
Diamicton	Particles of all sizes from clay to boulders	• Unsorted, no bedding structure • Essentially debris flow deposits	• High energy for transport – all material entrained • During high intensity storms that result in high-magnitude flooding, or in high gradient cave passages.
Thalweg	Coarse gravel, cobbles, and boulders armoring the bed of the stream	• A result of the winnowing of finer materials from channel facies deposits	• Requires a flowing stream with a moderate flow velocity during normal conditions
Channel	Sands, silts, and cobbles	• Typical cave stream deposits - make up most of the clastic sediment found in caves • At least partially sorted, but may be well sorted in a particular bed • Crudely stratified layers	• Transported primarily as bedload • Observed where more recent flow has eroded and exposed deposits in the stream bank • Partially sorted as moved through passage • Stratigraphy often discontinuous along a passage
Slackwater	Fine-grained deposits of silt and clay	• Usually top layer of clastic deposits • Often found in crevices and smaller niches in caves (less likely to have fast flowing water) • "Blanket-like deposits"	• Transported as suspended load in flow - requires low-energy for deposition out of suspension • Occurs either during ponding at high flood

		• In non-glaciated regions (i.e. Kentucky) clays and silts usually consist of quartz fines, dolomite/calcite silts, and other allogenic clay minerals dominating the surficial soil	levels or as floodwaters recede • Also may be sediment that was backflooded[1] into cave systems during a flood event on surficial rivers
Backswamp	Usually clay and fine silt, with some clastic fragments	• Insoluble material from limestone dissolution or infiltrated surficial soil	• Caves with large cross sections (wide passages), slow flowing water, and little sediment transport - hydraulically equivalent to an underground swamp

[1]*Backflooding refers to reversal of flow back into the cave system at groundwater springs and abandoned passages in adjacent river systems, occurring during flood events and especially in areas with rising base level (Farrant & Smart, 2011).*

These various types of facies and environments illustrate the different types of hydrological conditions that can exist in cave systems. Sedimentary structures such as ripple cross lamination can also be used to determine past flow direction(s) including regular stream flow, and reversing flow as a result of water forced upstream from locally reversed gradients (Farrant et al., 2014). A sedimentary succession including cut and fill deposits with lateral fining is a common deposit in a gentle vadose or shallow phreatic cave (Ford & Williams, 2007).

Integration of various data, including physical and chemical characteristics of sediment deposits in caves, sediment and contaminant time constraint data, and knowledge of historic activities on the surface, can therefore be used to understand sediment dynamics and contaminant accumulation within cave systems.

2. Study Site

2.1 The Central Kentucky Karst

The Central Kentucky Karst is a region of widespread karst located in the Horse Cave and Mammoth Cave National Park Area of Central Kentucky (Figure 1). Karst occurrence in Kentucky is extensive, and the Central Kentucky Karst has a high potential for karst development due to widespread deposits of Mississippian-aged limestone, capped with shales and sandstones (Paylor & Currens, 2001; KGS & UKy, 2012a). The Central Kentucky Karst is part of the Western Pennyroyal Region, and is characterized as a limestone plain with typical geomorphic karst features such as sinkholes, sinking streams, springs, caverns, and low-relief escarpment features (KGS & UKy, 2012b). The Green River is the major waterway in the area, flowing through Mammoth Cave National Park and draining over 23,900 km^2 (Carey, 2009).

2.2 Hidden River Cave

The majority of accessible Hidden River Cave passages are under the town of Horse Cave, Kentucky, USA, with the only known accessible entrance to the cave system in downtown Horse Cave (Figure 1). Horse Cave sits in a valley with a large escarpment 200-300 m in elevation to the northwest and is located 17 km southeast of Mammoth Cave National Park (Google Earth, 2017). Hidden River Cave is carved out of Mississippian-aged limestone deposits (Pohl, 1970; Blair et al., 2012), and is hydrogeologically related to Mammoth Cave (Kambesis, 2007). The cave system drains

the Gorin Mill Spring groundwater basin, which is a subbasin of the larger Green River basin (Ray & Currens, 1998; Carey, 2009). The Gorin Mill basin drains 395 km^2 into the Green River to the northeast, approximately 3.5 km upstream of Munfordville (Figure 1; Ray & Currens, 1998; Carey, 2009; Blair et al., 2012).

The Hidden River Cave system contains over 33 km of mapped passages (Gulden, 2016) and is an active, multi-level cave. Passage depths below the surface datum at the top of the slope to the cave entrance (195 m above mean sea level) reach approximately 50 meters below the surface (CRF & West, 2013), however precise depth measurements have not been made in this cave system. Lower level passages are closer to 50 m below the surface, while upper level passages are shallower with a depth of approximately 20 m below the surface. Hidden River Cave is a dark cave system, meaning there are no light sources or windows within the cave. Water flow in the cave system is directly related to rainfall events in the basin, with the cave experiencing episodic flood events multiple times per year (Foster, 2016). Lower level passages contain continuously flowing water year-round, while upper levels only experience flow during flood events. As such, upper level passages are often relatively dry, and may have stagnant pools remaining on passageway floors between flooding events. Water flow in lower levels is also seasonally dependent, and the amount of air space (i.e. distance from water level to ceiling) above the stream in a given passage is variable. From the cave entrance, the stream can be followed for approximately 100 m directly upstream (southwest) and 150 m downstream (east) of the entrance until it drops to a lower passage. The stream continues this pattern of appearance and disappearance and is intermittently accessible in the traversable

sections of the cave system, with flow diverted to lower passages in some sections. The cave system contains a variety of passage sizes, ranging from large domed rooms up to 34 m high and 70 m wide, to small, barely large enough for a person to fit. The primary rock visible in the cave is limestone, with some chert and calcite-rich speleothem deposits, and many passages contain piles of dislodged ceiling or wall materials (piles of debris, called breakdown).

2.3 The History of Horse Cave, Kentucky

The valley in which the town of Horse Cave lies was first settled in 1794 (Edwards & Edwards Gardiner, 1940). During the early 1800's, settlers continued to move into the Horse Cave area and by 1850 the first tobacco factory had opened, with town growth increasing more rapidly as the 1860's approached (Edwards & Edwards Gardiner, 1940; The Horse Cave Heritage Festival, 2002; Chaney, 2017). The first water works installation in the entrance of the cave was in 1887, and a stone dam that still exists today was built downstream of the entrance in 1890 to increase water delivery and to supply electricity for the growing town (Lewis, 1993). The cave was opened as a tourist attraction in 1916, offering tours downstream (southeast) of the entrance to a room called Sunset Dome and advertising the cave's impressive entrance and large population of blindfish (Lewis, 1993). From 1887, dependence on the cave stream as a town water source increased, especially when a drought occurred in 1930 (Lewis, 1993). As the town and economy grew, issues started to arise with contamination of the cave stream. For example, oil refinery waste was dumped into a sinkhole south of the cave system and

appeared at the cave entrance in 1931 (Lewis, 1993). A chlorinator was installed in 1932 to treat water due to the occurrence of typhoid amongst the population, and continued problems with the cave water quality provoked development of Rio Springs as an alternate water source, located northeast of Horse Cave on the north side of the Green River (Lewis, 1993). Industry, in addition to agriculture and tobacco growing continued to develop in the Horse Cave area, and with it population increased. Residential sewage was disposed of in septic fields or outhouses, and in some cases both residential and industrial waste were disposed of directly into sinkholes (Lewis, 1993). Hart County Creameries opened in 1941, and the dumping of whey waste into sinkholes combined with the existing cave stream contamination issues terminated the cave as a commercial tourist attraction by 1943 (Lewis, 1993; The Horse Cave Heritage Festival, 2002). The creamery remained in operation until closing in 1995 (The Horse Cave Heritage Festival, 2002).

The Horse Cave sewage treatment plant opened in 1964, disposing effluent into a sinkhole until it was clogged shortly afterwards, and thereafter disposing into the South Branch of the cave stream (Lewis, 1993). The newly constructed Cave City sewage treatment plant to the southwest also released effluent into a sinkhole that drained into the East Branch of the cave system (Lewis, 1993). The 1970 opening of Ken Dec, a chrome plating plant, added to the problems associated with sewage treatment (Manufacturer's News Inc., 1997). Located upstream of the cave system (Figure 1), the effluent from the chrome plating plant contributed two thirds of the total influent into the sewage treatment plant and overwhelmed the microbes involved in the treatment process (Lewis, 1993).

Hence, the sewage treatment plant effluent released into the cave system, which was already suffering from contamination issues due to the creamery waste, caused further degradation of water quality. Serious contamination of the cave system was first recorded at the entrance to the cave in downtown Horse Cave (Figure 1). Local history describes the horrible smell that emanated from the cave mouth. Local anecdotes discuss how the smell was so bad pedestrians would have to pass by the mouth of the cave on the opposite side of the street, referring to the cave as an open sewer (Kambesis, 2007; Chaney, 2016; Foster, 2016).

Industry continued to grow in Horse Cave, with several other manufacturing plants opening such as Dart Container Corporation in 1980, a Styrofoam container company, and more recently (in 2004 and 2007) specialty food manufacturers (Hart County Chamber of Commerce, 2014; Dart Container Corporation, 2017). The Styrofoam container company had an accidental spill in the early 2010's that released millions of Styrofoam beads 1-3 mm in diameter into the cave system (Foster, 2016). The beads are still visible on the cave ceilings and walls in certain passages (Figure 2) providing a further example of how industry has impacted the subsurface environments of Horse Cave.

The American Cave Conservation Association relocated its headquarters to Hidden River Cave in 1987, with the intentions of restoring the cave system and opening a museum and educational center (ACCA, 2013). In 1989, new sewage treatment plants opened in both Horse Cave and Cave City, and the cave system has been steadily

recovering since (Lewis, 1993; ACCA, 2013). The cave reopened as a tourist attraction in 1993, and continues to operate as such at the present-day (Lewis, 1993; ACCA, 2013).

Figure 2: Styrofoam beads 1-3 mm in diameter stuck to the ceiling (approximately 2 m high) of Wheet River passage (Figure 3). Styrofoam beads were transported through the cave system in an accidental spill from the Styrofoam Container Company (Dart) in the early 2010's, and remain visible on the ceiling and in crevices in Wheet River passage, and in Sunset Dome. Photo by Russ Ellis.

In 2010, there was a US Environmental Protection Agency lawsuit against Ken Dec, the original chrome plating plant. The company was found guilty of illegally disposing of untreated electroplating wastewaters between January 2004 and January 2009 (US EPA, 2017). The untreated wastewater would have entered the cave system either as sewage treatment plant effluent or from direct infiltration. The US EPA (2017) cites that the case resulted in the former Ken Dec plant manager being sentenced to 18

months in prison and a three-year term of supervised release on probation. Additionally, the company (Ken Dec) was fined $700,000 by the federal government, and paid a $95,000 restitution fine to the Caveland Environmental Authority for reimbursement of costs associated with cleanup and disposal of the metal waste (US EPA, 2017). Ken Dec was closed, and a new chrome plating plant later opened with proper waste disposal practices (Foster, 2016).

This study will attempt to determine whether anthropogenic impacts, such as the Ken Dec contamination, are recorded and can be identified within the sedimentary record of a cave system. This requires the collection and analysis of cave sediment from various locations in the cave system to both identify anthropogenic contaminants and to examine their spatial distribution to determine the processes that may be affecting their transport and deposition.

3. Methods

Detailed notes on the cave environment including passage morphology and water conditions were taken throughout the traversed passages of the Hidden River Cave system over the course of multiple visits during August 2015, May 2016, August 2016, and February 2017. Due to the nature of the cave system some areas are not accessible for sampling of any type due to unsuitable collecting conditions. Particular attention was given to the identification of potential sampling sites (Figure 3), which reflect the extent of visited passages within the system. Water sample, surface sediment samples, and

sediment cores were collected for physical and chemical analyses including sedimentology, chronology, and x-ray fluorescence using an ITRAX Core Scanner.

Fieldwork activities are limited to equipment the field team can carry in and out of the cave system. The varied sizes and logistics of accessing certain passages also limit the size of equipment that can be brought into the cave.

3.1 Sampling

Water and surface sediment sampling sites were selected in order to obtain samples that were likely to contain a record of contamination and also to provide a large areal spread within the cave system (Figure 3). Coring locations were chosen to coincide with concurrent collection of water and surface sediment samples, as well as to give a relatively even distribution throughout the cave system (Figure 3). Sediment cores were collected in 5-cm diameter PVC pipe using a push core method established in studies conducted in the Sac Actun Cave system in Quintana Roo, Mexico (Collins et al., 2015). Specific coring sites were chosen based on the presence of an adequate thickness of sediment (> 15cm), at various locations and levels within the cave system. Sampling occurred at different levels within the cave system as upper level passages would only experience flow during flood events, and should capture a record of flood events within sediment deposits. Sediments accumulating in lower level passages should record greater continuity of flow. Cave level is noted for sediment cores of interest discussed (see section 4). Sampling locations were also chosen to obtain samples in a variety of passage sizes to capture variation in transport processes with respect to passage size and

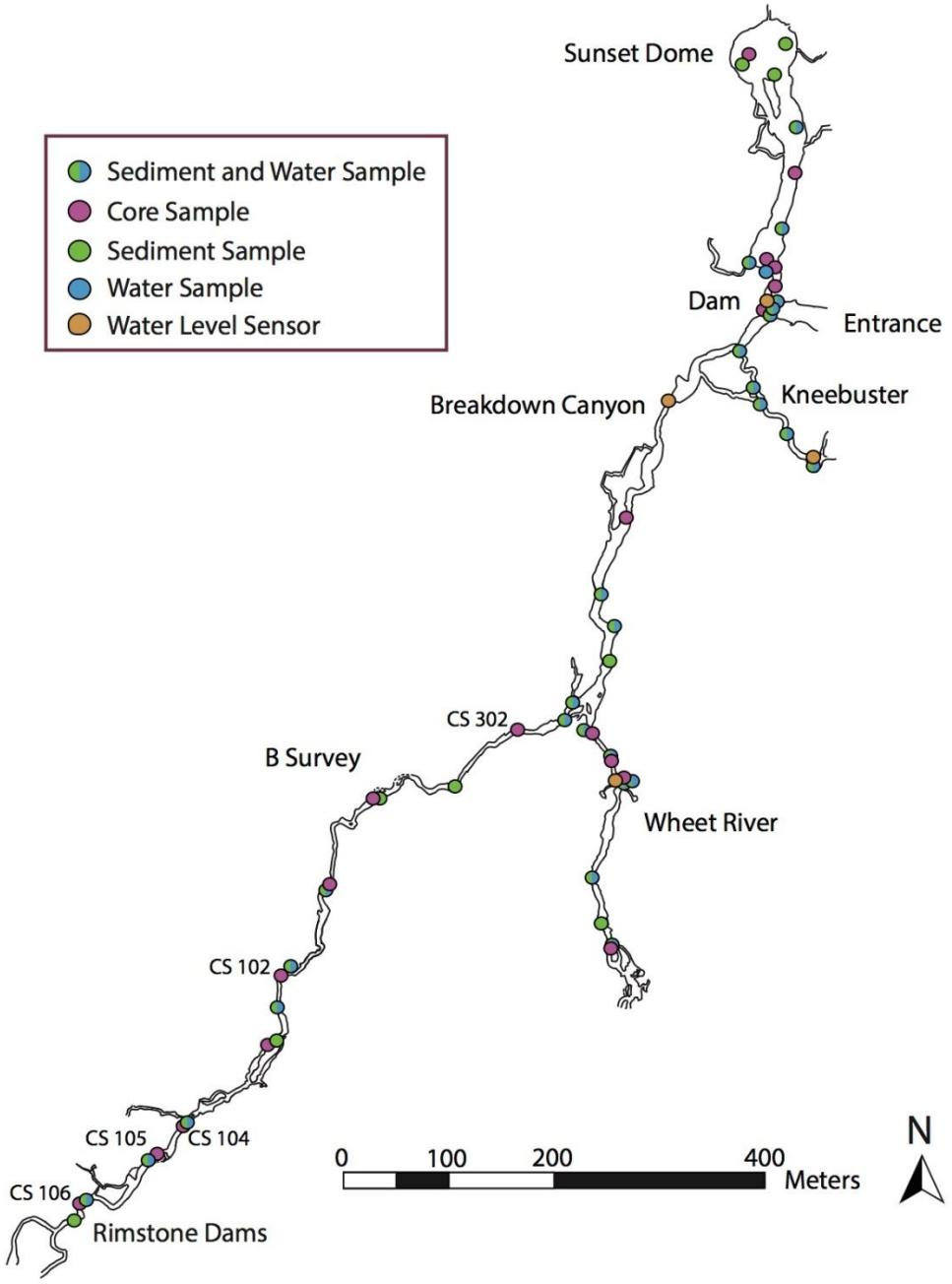

Figure 3: Truncated Hidden River Cave Map showing sampling locations within the cave system. Water, sediment, and core samples are indicated as blue, green, and pink dots, respectively. Water sensor locations are indicated in orange. Water flow in the cave system moves in a northeast direction (see Figure 1). Labels indicate local nomenclature for passages or locations within the cave system. The South Branch (see Figure 1) of the cave system drains through the B Survey and towards the entrance, joining with the East Branch (see Figure 1) of the cave stream. Core samples discussed in this study (CS 106, CS 104, CS 102, and CS 302) are labelled. *(Cave passages map modified from CRF & West, 2013)*.

changing water flow hydraulics (Figure 3). Site-specific characteristics were also noted, such as areas of topographic and geomorphological interest for context during later analyses. When possible, sites that were expected to be clay-rich were chosen for sampling as fine-grained sediment is required for Lead-210 dating. Ranging in length from 16-81 cm, twenty cores were cut in half, logged, and prepared for analysis.

Known passages within the Hidden River Cave system are completely mapped. However, the map obtained likely has errors due the limited methodology of mapping underground and out of satellite reception. Additionally, it is difficult to simply know precisely where or how far underground one is at any given time again due to the lack of satellite tracking signals underground. As a result, locations within the cave system and on the map are less precise than traditionally used in surficial studies.

3.2 Sediment Core Analysis

Cores were logged, and grain size interpreted using a grain size card in conjunction with the physical feel of the sediment. Cores were cut in half and the faces were cleaned and smoothed in preparation for a Cox ITRAX core scanner, which obtained elemental concentrations (through x-ray fluorescence), magnetic susceptibility, radiography, and high-resolution photography. The resulting elemental data were analyzed for select metals, chosen based on their relevance to surficial land use processes and potential contamination in the drainage basin (see Table 2). Relative metal concentrations were recorded in total counts at 200-micrometer intervals using a Mo X-ray source**.** Metal values are reported in relative concentrations (total counts) as standard

metal concentration data for Hidden River Cave are not available (c.f. Gregory et al. (2015)).

Table 2: Justification for metals chosen for further analysis.

Metal	**Justification**
Chromium	• Historical dumping from a previous metal plating plant upstream of cave system • Cr (III) and Cr(VI) present in metal plating effluent (Tenorio & Espinosa, 2001; Hunsom et al., 2005) adsorbs to clay minerals, degrading sediment quality and increasing toxicity to the ecosystem (Bradl, 2004)
Copper	• Historical dumping from a previous metal plating plant upstream of cave system • Presence in metal plating effluents (Tenorio & Espinosa, 2001; Hunsom et al., 2005) • Copper preferentially adsorbs onto organic matter associated with the clay fraction of deposits, and can also be adsorbed by carbonates (Bradl, 2004)
Nickel	• Historical dumping from a previous metal plating plant upstream of cave system • Presence in metal plating effluents (Tenorio & Espinosa, 2001; Hunsom et al., 2005) • Adsorbs to clays (McLean & Bledsoe, 1992)

3.2.1 Chronology

3.2.1.1 Radiocarbon (^{14}C)

Core CS 105 was sampled for radiocarbon dating due to the presence of testable organic material (charcoal and bulk carbon) found distributed throughout the core. A total of 3 samples in 1-cm sections were sampled from the full diameter of the open core face at 19, 39 and 64 cm depth below surface (see section 4.1.2.1, Table 4). Samples at 19 and 39 cm depth were analyzed for charcoal, and the sample at 64 cm was analyzed for bulk carbon (see section 4.1.2.1, Table 4). Results were analyzed at the Direct AMS labs in

Bothell, Washington (USA) and returned corrected for isotopic fractionation with $\delta^{13}C$ values measured on an accelerator mass spectrometer. Radiocarbon dates are reported as Radiocarbon Age Before Present with a 1σ error as standard deviation (see section 4.1.2.1, Table 4).

3.2.1.2 Lead-210

Core CS 302 was selected for Lead-210 analysis due to its high clay content and its location on a cave bank where there is a relatively high potential for a continuous sedimentary record to be preserved (Ford & Williams, 2007). CS 302 was sampled and samples were sent to MyCore Scientific in Dunrobin, Ontario (Canada) for Pb-210 dating. A total of 12 samples, each in 1-cm sections, were sampled from half of the open core face and dried in preparation for analysis. Ten of 12 samples were from the top 20 cm of the core (see section 4.1.1.1, Table 3). The dates obtained from these samples are for the top of each analyzed 1-cm section, beginning from 0 cm at the top of the core (see section 4.1.1.1, Table 3). MyCore Scientific determined Pb-210 concentrations in the core using the constant rate of supply (CRS) model of accumulation where Pb-210 concentrations change based on the amount of radioactive decay that has occurred in the sample. This can be used to determine the age of the sample and sediment accumulation rate (Appleby et al., 1979; Appleby & Oldfield, 1983; Ghaleb, 2009). Pb-210 dating measures the amount of Pb-210 that is in excess of Radium-226 (in Becquerels per gram (Bq/g)), which is typically 10 – 50 times in excess at the top of a core (Appleby & Oldfield, 1983; Ghaleb, 2009). Pb-210 is a naturally occurring radioisotope, and excess amounts of Pb-

210 decrease down the core due to radioactive decay, until there are negligible amounts in comparison to background Radium-226 values (Ghaleb, 2009). As such, older sediment will contain less Pb-210. Lead has a half-life of 22.3 years, and is suitable for dating sediment over a time of approximately 120 years (Ghaleb, 2009). The Pb-210 profile in core CS 302 conformed well to the exponential CRS model, meaning that the reported dates are likely to be reasonably accurate. Sediment accumulation rates were estimated on the basis of the Pb-210 dates obtained by using a linear interpolation process in a similar fashion to that followed by Webb & Webb (1988). Standard deviation for interpolated values was determined by applying the formulas used in the Excel spreadsheet by MyCore Scientific for non-interpolated dates, which accounts for the difference in excess Pb-210 in samples relative to the sample at the top of the core (i.e. year of coring, 2016).

Errors associated with Pb-210 dating include measurement errors in weighing, radiochemical extraction, and radionuclide counting in the lab (MyCore Scientific Inc., 2017). The standard deviation values calculated for the dates take into account this error, as well as uncertainties in the age model calculation. The amount of uncertainty associated with the dates obtained increases with depth in the core due to smaller Pb-210 concentrations in comparison to background levels of Pb. The background levels of Pb have not remained constant over time and have increased substantially in the twentieth century due to coal burning, industrialization, and use in gasoline (Jackson et al., 2004; Shotyk & Krachler, 2010). Pb use in gasoline was subsequently banned in Western countries in the later part of the twentieth century, causing a reduction in atmospheric Pb (Jackson et al., 2004) and again changing the background signal. These changes in

background levels of Pb may cause errors in Pb-210 age calculations if not accounted for properly.

3.3 Water Level Sensors

Reefnet Sensus Ultra™ Dive Recorders were used to record changes in water depth in select locations within the cave (Figure 3) to inform the occurrence of flood events, and therefore sediment transport events. The dive recorders record changes in absolute pressure and temperature. Upon data download into the proprietary computer software, these pressure changes are converted into a value reflecting water depth. Sensors were set to a threshold value of 1015 millibars (mbar) based on the average ambient absolute pressure of 995 mbar at the entrance to the cave. It is after the device reaches the threshold pressure that it starts to record pressure changes. A threshold value of 1015 mbar, 20 mbar over the ambient pressure, is equivalent to an increase in depth of 20 cm of freshwater (Reefnet Inc., 2006). Sensors were set to record at 10-second intervals once water depth surpassed the threshold for recording.

Sites for installation of the sensors were chosen based on areas known to experience flooding or areas that are underwater for the majority of the year. Breakdown Canyon (Figure 3**)** was chosen due to its narrow morphology in comparison to passages up- and downstream. The narrowing of the channel at Breakdown Canyon results in locally higher water levels during flood events, making it an appropriate sensor location for recording flood events. The reasoning for placing a sensor immediately upstream of the dam near the cave entrance (Figure 3) is similar. The cave entrance experiences high

floodwater levels two to three times per year on average (Foster, 2016) making it an ideal area to place a sensor. Sensors located at the Wheet River Beach and in a pool near the end of the Kneebuster passage (Figure 3) were both placed in pools with low flow that is almost unnoticeable to an observer. Sensors were placed in pools at the upstream ends of passages since they are likely to experience and record higher flood water levels. Sensors were left recording in the cave for 6 months during the fall and winter seasons (2016-2017), which in central Kentucky average 11 degrees Celsius and receives 579 mm of precipitation from September – February (NOAA, 2017a, b). The winter season averages 4 degrees Celsius with 445 mm of precipitation from December – March (NOAA, 2017a, b).

Unfortunately, the water level sensor at Breakdown Canyon (Figure 3) was the only sensor of four that recorded data for the duration of placement in the cave. The pressure threshold was set based on initial ambient pressure measured at the cave mouth. Setting the pressure threshold based on an ambient pressure reading at the mouth of the cave was likely inaccurate since this area may experience fluctuations in microclimate (including ambient pressure) due to interaction with the surface (Pflitsch et al., 2010). The ambient pressure may be different further into the cave away from the effects of the entrance. Therefore, the selection of a 1015 mbar threshold (i.e. at what water depth to start recording) may not have accurately reflected a 20 cm increase in water depth making the results inaccurate and unreliable.

4. Results

The analytical results for five of 20 sediment cores sampled are presented, with observations of lithology (including grain size), colour, core lamination characteristics, relative metal concentration trends, and radiocarbon and lead-210 dating results (Figures 4, 6, 8-11); Tables 3, 4). Core CS 302 is particularly important as lead-210 dates were obtained for the upper part of this core (Table 3). Cores discussed are all from the B Survey passage, and represent a sequence of settings from most upstream (closer to industrial area on land surface) to most downstream (closer to entrance) within the cave system.

4.1 Sediment Cores

Sediment size in logged cores ranges from clay to upper-medium sand (Figures 4, 6, 8-10). Observed facies included massive sand (Sm), massive fines (clay and silt; Fm), laminated fines (clay and silt; Fl), interbedded fines and sand (Sh, Fl), and horizontally laminated sand (Sh). Both gradational and sharp contacts are present between facies types. Variations and trends in the relative concentration of the metals analyzed using the ITRAX core scanner are described. The analytical results for each of the five cores analysed in detail are described below.

4.1.1 Core CS 302

Core CS 302 was taken from a bank in the B Survey passage (Figure 3) approximately 6 m wide and 5m high. The walls of the passage were undulating with sediment caked onto them. This is consistent with areas of the cave prone to periodic

flooding. The sampled bank was 4 m wide x 3 m tall, and in the upper level of the cave downstream of the industrial area on the ground surface. The sediment in core CS 302 is dominated by clay to silt grain sizes, with massive (Fm) and laminated fines (Fl) facies types. The core photo shows an irregular series of distinct laminae and thin beds ranging from 1 – 20 mm thick with both gradational and sharp contacts (Figure 4). The sediment below 200 mm from the top of the core, shows a distinct change in sediment colour from a medium brown to a red colour.

The results of an ITRAX scan were plotted for selected metals associated with past contamination events (chromium, copper and nickel; Figure 4) in a similar manner to those presented by Miller et al. (2015), and Lintern et al. (2016) for contaminated lacustrine and fluvial sediments. Figure 4 shows relative metal concentrations for CS 302 alongside the ITRAX photograph and sediment log. The core plot displays relatively consistent values for copper, chromium and nickel from the bottom of the core up to approximately 40 mm from the top (Figure 4). Metal total counts values slowly increase in the upper 40mm of the core until they reach maximum values at approximately 15 mm from the top (Figure 4). The relative concentration of each metal then decreases in the upper 15 mm of the core, where the total counts values revert almost to the levels observed below 40 mm (Figure 4). However, the relative concentration of nickel shows another peak in values at approximately 8 mm below the top (Figure 4).

4.1.1.1 CS 302 Lead-210 Results

Results obtained from lead-210 dating analysis are shown in Table 3 (also Figure 11). There was a large excess of Pb-210 (> 0.06 Becquerels per gram (Bq/g)) over the Ra-226 background values of 0.033 Bq/g in the top 20 cm of this core, making it suitable for dating. Uncertainties in dates are over 20% in the core sections below 14 cm due to smaller lead-210 excess (<0.06 Bq/g) over background Ra-226 values.

Table 3: Lead-210 lab results for sediment sampled from core CS 302. Standard deviation for interpolated values was determined by applying the formulas used for the non-interpolated dates.

Depth in core	Pb-210 Age (year)	STD (years)	Notes
0 cm	2016.6	0	
1 cm	2007	0	Interpolated
2 cm	1998	2	
3 cm	1993	2	Interpolated
4 cm	1985	3	
5cm	1973	4	Interpolated
6 cm	1960	11	
7 cm	1950	16	Interpolated
8 cm	1939	33	
9 cm	1930	36	Interpolated
10 cm	1918	47	
11 cm	1910	-	Interpolated

Core CS 302 was taken from a bank on the side of a passage (Figures 3, 5) under the assumption that it would contain fine-grained material (< 150 micrometers) suitable for Pb-210 dating and to correlate relative metal concentrations with both historic events and other core samples since it is the furthest downstream core sample that was analyzed. Based on Pb-210 dating results (Table 3), there appears to have been an accumulation of 10 cm of sediment in a 98 year period (1918-2016). It can therefore be estimated that

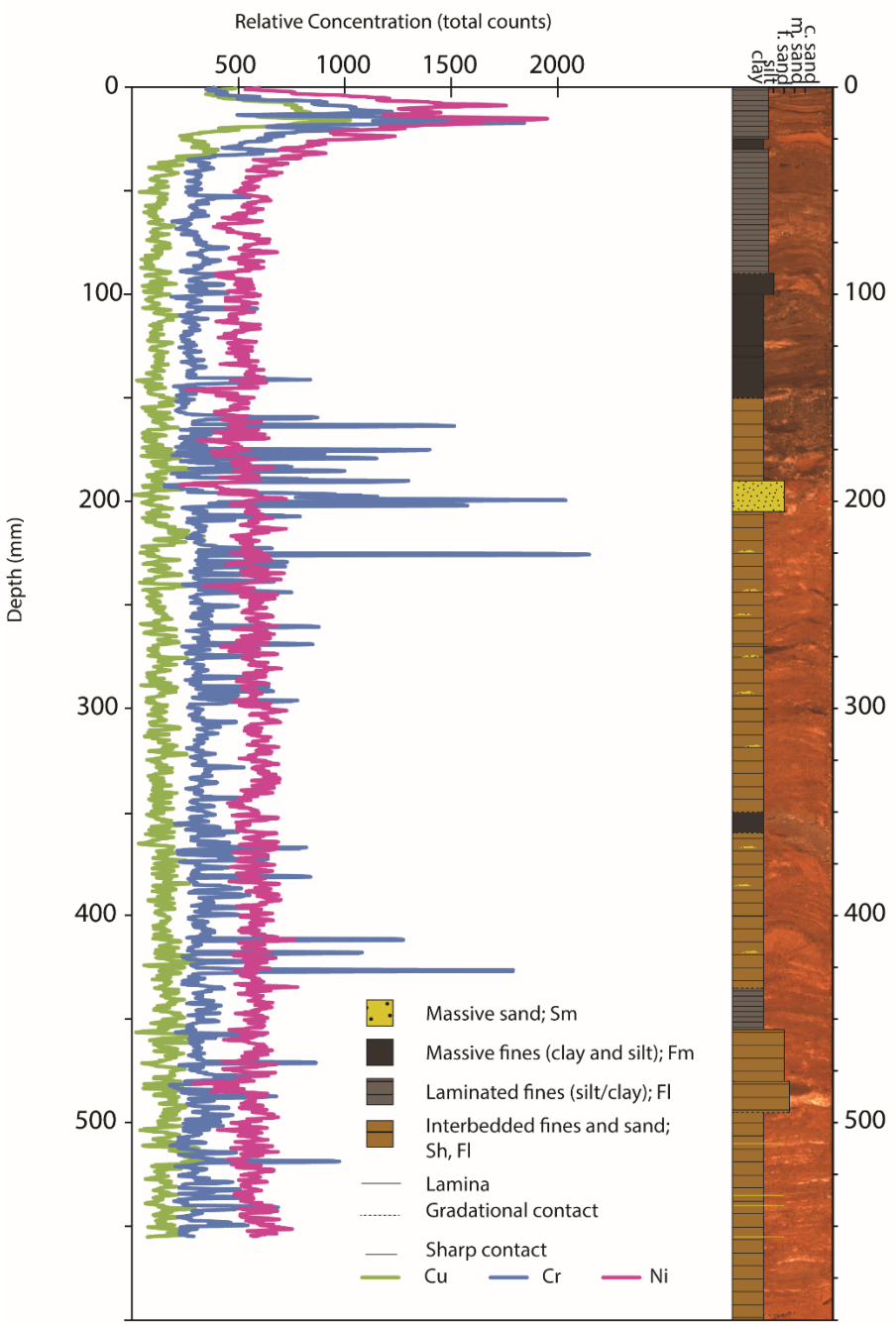

Figure 4: Core sample CS 302 ITRAX elemental data plotted with core image and sedimentological log. Elemental data is shown on the left with depth in the core (millimeters) on the y-axis and relative metal concentration in total counts on the top x-axis. An average range of 5 values (= 1 mm rolling average) was used to plot the metal data. Relative concentrations of copper (green), chromium (blue) and nickel (pink) are displayed for the full length of the core. The photographic image on the right displays the core overlain to the left with a sedimentological log. Core CS 302 is the furthest downstream core analysed in this study and was sampled from a bank in a passage in the B Survey in the upper level of the cave system.

sediment accumulation in the CS 302 location is approximately 1 mm per year or 1 cm per decade.

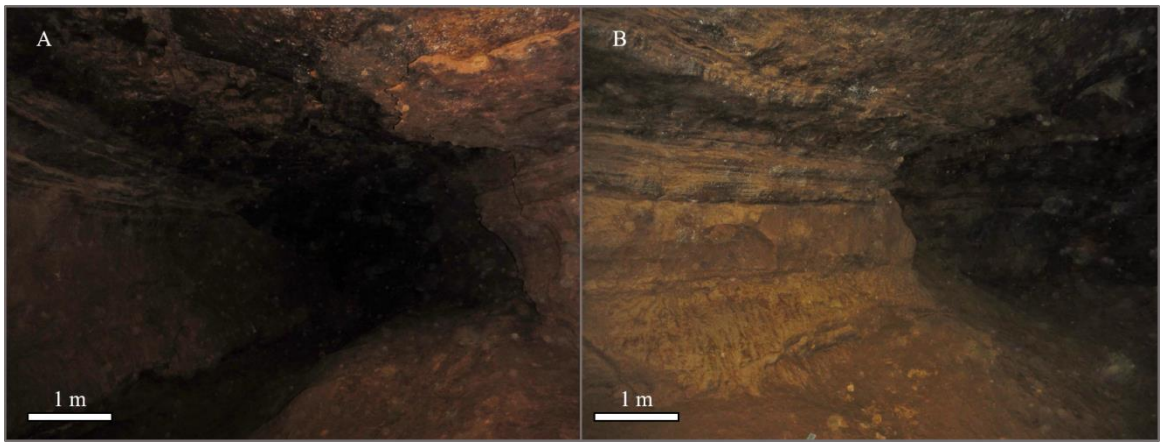

Figure 5: Core CS 302 sampling location photo (B Survey passage, Fig 3). The passage is approximately 4.5 m wide and is on the cave's upper level. A) Looking upstream from the coring location. The bank from which the core was taken is 4 m wide and 3 m tall and can be seen on the right of the photo. B) Looking downstream from the coring location, with the bank from which the core was taken on the left of the photo. Blemishes on images are due to high moisture content in the cave air, and have been removed where possible.

4.1.2 Core CS 105

Core CS 105 was taken in a cave passage just above a pool (Figure 6). The passage is narrow (1-2 m wide) at the base and widens at a height of approximately 1 m above the base. This passage also displays scalloping on the walls above 1.5 m, presumably resulting from periodic water flow (Figure 6). The CS 105 core contains sediment ranging in size from clay to medium sand, with over 50% of the core consisting of sand-sized grains (Figure 6). The core contains sharply interbedded and laminated sediment with laminae thickness typically less than one mm.

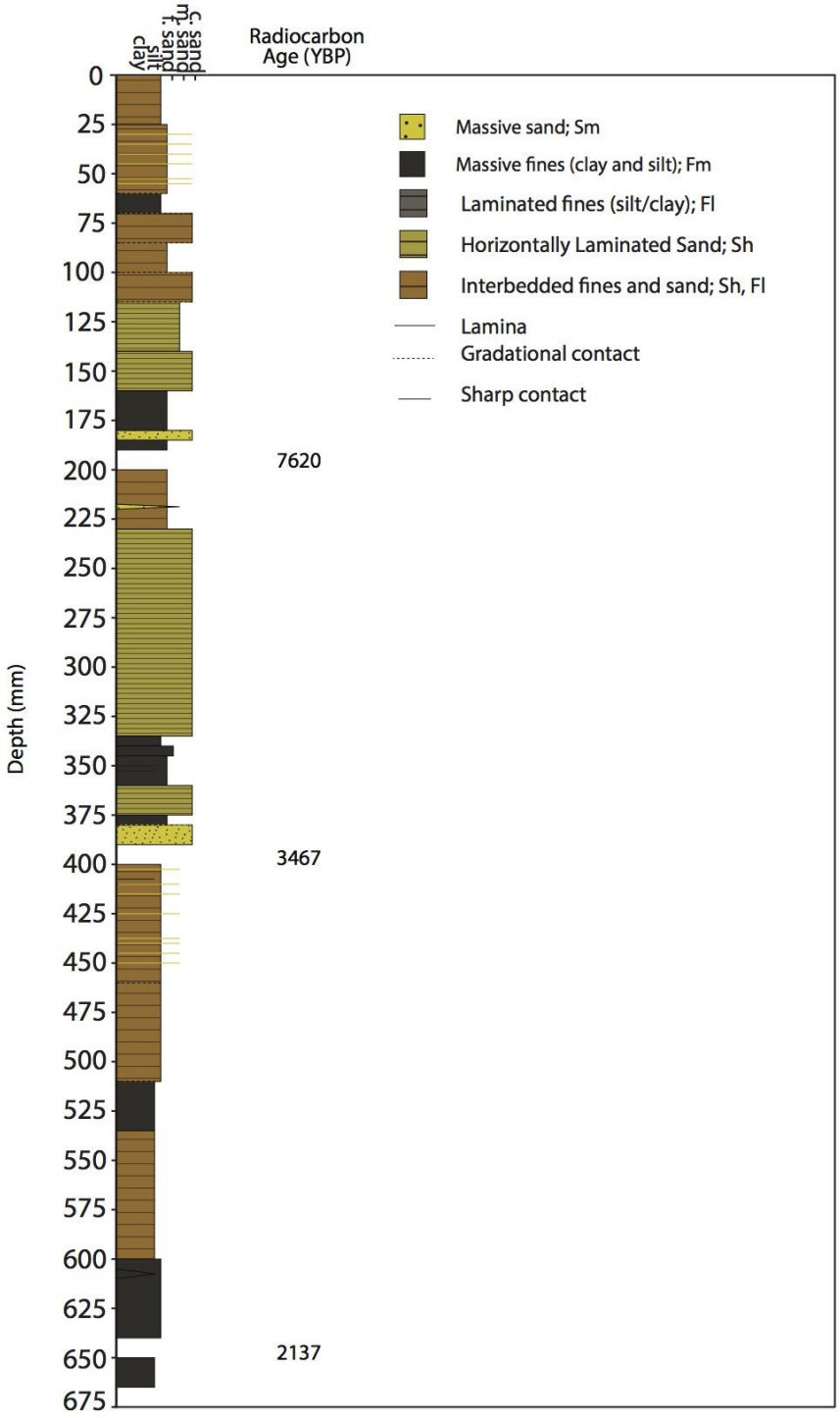

Figure 6: Core sample CS 105 sedimentological log. Core CS 105 samples were sent for radiocarbon dating, with results from 1-cm sections indicated in the 'Radiocarbon Age (YBP)' column. Core CS 105 was taken from a B Survey passage on the upper level of the cave system.

Figure 7: This photo shows the sampling location of CS 105, a passage in the B Survey passage with a wall morphology similar to a cut bank. The passage can be vertically divided into three sections; from the floor to 1 m high is a 1-2 m wide terrace; an incised wall section lies between 1 – 1.5 m; and above 1.5 m the passage wall has a concave scallop-like morphology created by water flow. *Photo by Russ Ellis.*

4.1.2.1 CS 105 Radiocarbon Results

Radiocarbon dating analysis of organic material collected from CS 105 returned age results ranging from 2137 – 7620 years before present. It was expected that ages would increase with depth, but radiocarbon results did not display this trend (Table 4). The expected oldest sample taken from a depth of 64-65 cm in the core was dated as bulk carbon, and returned the youngest age at 2137 years before present (YBP). The expected youngest sample from 19-20 cm from the top of the core was dated as charcoal and returned the second oldest date at 3467 YBP.

Table 4: Radiocarbon Dating lab results. Ages are given as years before present, with standard deviation as 1σ error. Results include actual age order based on returned radiocarbon dates.

Depth in core	Radiocarbon age		Radiocarbon Dated age order
	Years Before Present	1σ error	
19-20 cm	7620	35	2
39-40 cm	3467	27	3
65-65 cm	2137	28	1

Unfortunately, the radiocarbon age order for the CS 105 samples was not in the expected chronological order with respect to depth (Table 4), and as such did not complement sediment accumulation rate calculations. One potential explanation for this is that pre-existing charcoal and bulk carbon material was washed in from the surface, or that a large amount of mixing occurs within the system. As such, the radiocarbon dates likely do not represent the age of the sediment itself.

4.1.3 Cores CS 106, 104, and 102

Cores CS 102, CS 104, and CS 106 are discussed together as only ITRAX data, and not chronology data were analyzed for these cores. Maximum total counts values decrease in cores in the order CS 104, CS 102, 106, and 302 (Table 5).

4.1.3.1 Core CS 102

CS 102 contains grain sizes of clay to upper-medium sand, and predominantly silty-clay with some sandy beds and laminae. Sequences of laminae form the facies interbedded fines and sand (Sh, Fl). Most contacts between laminae are horizontal and gradational, with some sharp contacts. CS 102 (Figure 8) contains chromium, nickel and copper peaks in the upper portions of the core above 40 mm (Table 5). Like CS 302, CS 102 also changes colour from medium-brown to red below 60 mm. The maximum metal peaks between 15-25 mm occur above observed sediment colour change depth of 60 mm (Table 5).

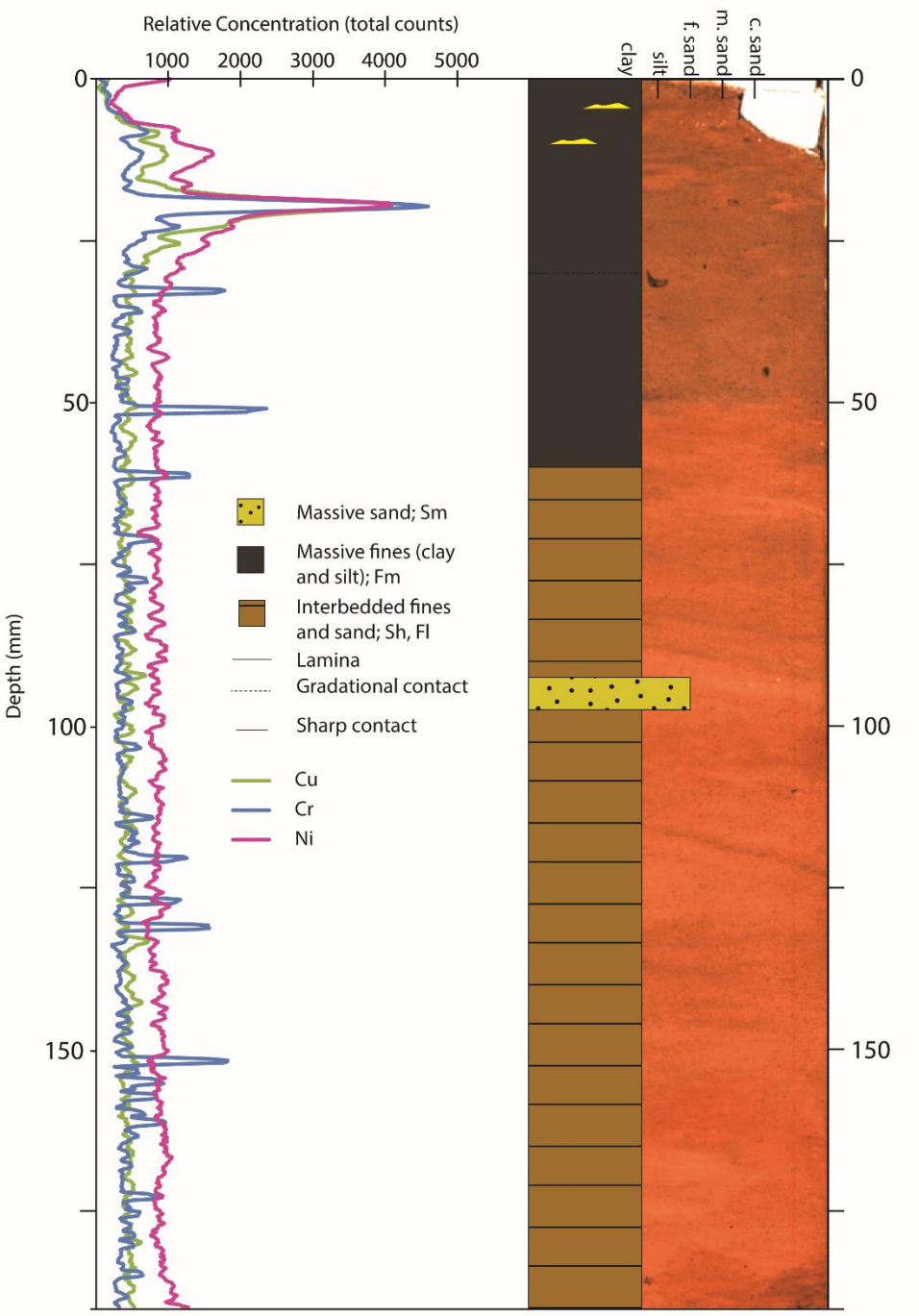

Figure 8: Core sample CS 102 ITRAX elemental data plotted with core image and sedimentological log. Elemental data is shown on the left with depth in the core (millimeters) on the y-axis and relative metal concentration in total counts on the top x-axis. An average range of 5 values (= 1 mm rolling average) was used to plot the metal data. Relative concentrations of copper (green), chromium (blue) and nickel (pink) are displayed for the full length of the core. The photographic image on the right displays the core overlain to the left with a sedimentological log. Core CS 102 was taken from the B Survey in the lower level of the cave.

4.1.3.2 Core CS 104

CS 104 contains grain sizes of clay to upper-medium sand, with overall more equal proportions of fine and sandy grains in comparison to other analyzed cores. Sequences of laminae form the facies laminated fines (silt and clay, Fl), horizontally laminated sands (Sh), and interbedded fines and sand (Sh, Fl). Most contacts between laminae are horizontal and gradational, with some sharp contacts. CS 104 (Figure 9) contains peaks in chromium, nickel and copper, in the middle of the core record (between 125-150 mm) rather than the upper portion like the other cores (Table 5). CS 104 does not display the medium-brown to red colour change, however is overall coarser (medium sand) above 120 mm (Figure 9; Table 5).

4.1.3.3 Core CS 106

CS 106 contains grain sizes of clay to upper-medium sand, with predominantly silty-clay with some sandy beds and laminae. Sequences of laminae form the facies laminated fines (silt and clay, Fl), horizontally laminated sands (Sh), and interbedded fines and sand (Sh, Fl). Most contacts between laminae are horizontal and gradational, with some sharp contacts. Core CS 106 (Figure 10) contains chromium, nickel and copper peaks above 25 mm in the upper portions of the core (Table 5). Similar to CS 302 and CS 102, sediment in CS 106 changes colour from medium-brown to red below 90 mm. Maximum metal peaks occur above this observed sediment colour change depth of 90 mm (Table 5).

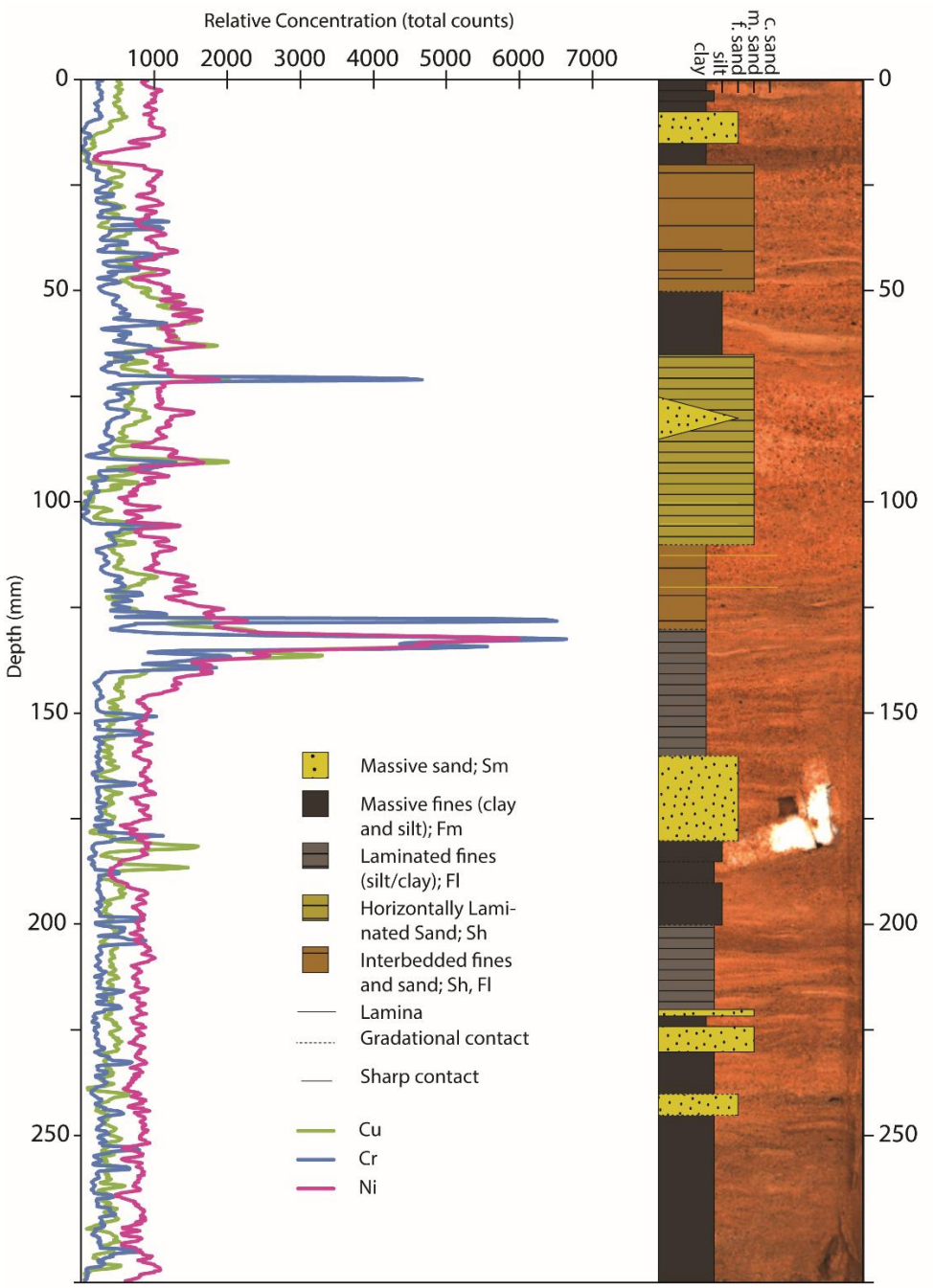

Figure 9: Core sample CS 104 ITRAX elemental data plotted with core image and sedimentological log. Elemental data is shown in the graph on the left with depth in the core (millimeters) on the y-axis and relative metal concentration in total counts on the top x-axis. An average range of 5 values (= 1 mm rolling average) was used to plot the metal data. Relative concentrations of copper (green), chromium (blue) and nickel (pink) are displayed for the full length of the core. The photographic image on the right displays the core overlain to the left with a sedimentological log. CS 104 was taken from a topographic low in the B Survey passage on the upper level of the cave.

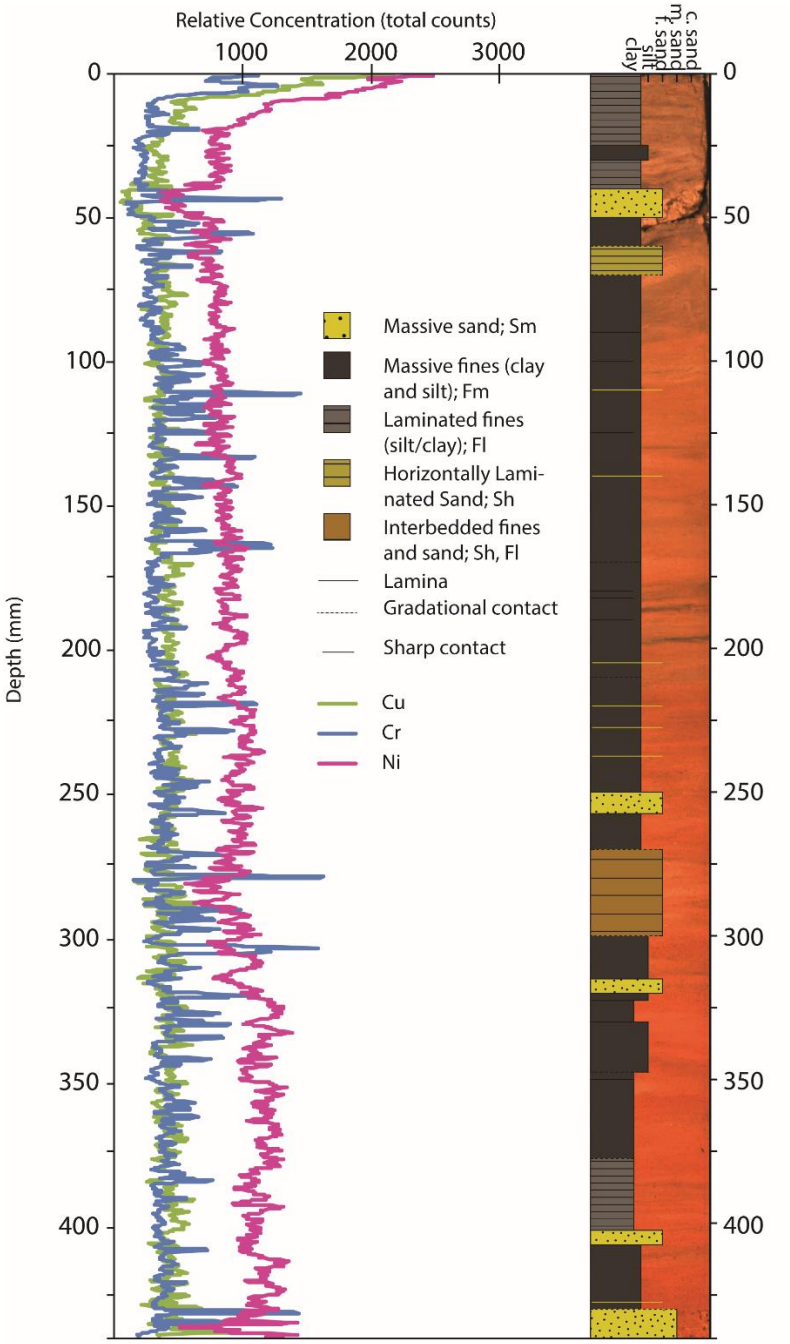

Figure 10: Core sample CS 106 ITRAX elemental data plotted with core image and sedimentological log. Elemental data is shown on the left with depth in the core (millimeters) on the y-axis and relative metal concentration in total counts on the top x-axis. An average range of 5 values (= 1 mm rolling average) was used to plot the metal data. Relative concentrations of copper (green), chromium (blue) and nickel (pink) are displayed for the full length of the core. The photographic image on the right displays the core overlain to the left with a sedimentological log. Core CS 106 is the furthest upstream core in this study and was sampled from the Rimstone Room on the lower level of the cave.

Table 5: Summary of observation for cores CS 106, 104, 102, and 302. Cores are ordered from most upstream (closer to industrial area on land surface) to most downstream (closer to entrance) and are all from the B Survey passage (see Figure 3 for sampling map). Colour change indicates the depth at which there is a distinct change from medium-brown to red in sediment colour moving down the core. Peak metal total counts values from ITRAX data are indicated with depth in total counts. Grain size is noted as per the sedimentological logs, and also included is a sampling site description.

Core and total core length	Colour change	Highest Metal peaks			Grain size	Sampling Area
		Metal	Depth from top of core	Total counts value		
106 **440mm** **Figure 10**	90 mm	Cr	0.4 mm	1645	-Mostly clay-silt -Some fine sand lamina and thin beds	Rimstone dams, large room with low ceilings (<1.5 m) lower level of cave; directly below industrial area on surface
		Ni	0.4 mm	2498		
		Cu	0.4 mm	1315		
104 **265mm** **Figure 9**	None but coarser >110-120 mm	Cr	132 mm 127 mm 70.8 mm	6648 6445 4673	-Interspersed clayey-silt and fine-medium sand beds or lamina	In topographic low beside a pool, upper level of cave; on downstream edge of industrial area on surface
		Ni	132 mm	5559		
		Cu	132 mm	5995		
102 **190mm** **Figure 8**	60 mm	Cr	19.6 mm	4602	-Mostly clay-silt -Some fine sand blobs and a fine sand lamina	Dome area in topographic low, lower level of cave; downstream of industrial area on surface
		Ni	19.4 mm	4087		
		Cu	19.6 mm	4082		
302 **595mm** **Figure 4**	200 mm	Cr	15-18 mm	1934	-Mostly clay-silt -Some fine-medium sand very thin beds	Bank in B Survey passage ~4.5m feet wide; bank 4m wide x 3m tall, upper level of cave; downstream of industrial area on surface
		Ni	10-18 mm	1950		
		Cu	8-18 mm	1019		
		Zn	12.4 mm	2517		

5. Discussion

Hidden River Cave is an active, multi-level cave system that experiences continuous water flow in parts of the cave year-round. This water flow results in variable amounts of sediment transport throughout the cave system. Since water levels in the cave have been recorded to show a direct relationship to rainfall events in the basin (Foster, 2016), the cave also experiences episodic flood events that allow the transport and deposition of greater amounts of sediment, particularly in upper levels of the cave. Patterns of sediment movement within the cave can be used to understand how potential contaminants may move through the system and other connected groundwater systems. Potential contaminants may also be deposited on upper levels of the cave during flood events and may be re-suspended during subsequent floods, effectively re-distributing the contaminants. Understanding sedimentation patterns in such a cave system requires analysis of sediment types (Figures 4, 6, 8-10) and their location of deposition as well as an understanding of sedimentation rates (Tables 3 and 4). In this study information on sedimentation rates was obtained by dating the sediment within sampled cores using radiocarbon and Pb-210 methodologies and is key to interpretation of sediment deposits.

5.1 Sedimentation Patterns and Depositional Processes

Banks of sediment found at the sides of cave passages are deposited as floodwaters are waning (Ford & Williams, 2007). As water level decreases, energy at the

side of the passage will decrease first causing deposition of fine-grained sediment close to the passage walls (Ford & Williams, 2007).

There is large variation in sediment transport and accumulation rates in cave systems, dependent upon factors such as the cave system's hydraulic characteristics (Ford & Williams, 2007). Sediment transport within cave systems is largely episodic (Newson, 1971; Bosch & White, 2004; Plotnick et al., 2009), particularly in upper level passages that do not experience regular flow. Core CS 302 was collected from a marginal bank in an upper level passage which only experiences flow during larger flood events, and the sediment sampled at this location may have accumulated during waning flood flows. The CS 302 core (Figure 4) shows gradational contacts between facies, and some sharp contacts associated with a change in grain size between fine sands and clay or silt. This interbedded coarse and fine material (Figure 4) can be attributed to the waning flow of a flood event. In reducing energy conditions, fine sands are deposited out of suspension before silts and clays, resulting in the interbedded deposit (Ford & Williams, 2007). The change from fine sand to silts and clays appear to indicate a more abrupt change in flow energy.

In each of the cores 102, 104 and 106 (Figures 8-10), taken upstream of CS 302 (Figure 3), sediment beds and laminae consist of laminated fines (silts and clays, Fl), horizontally laminated sand (Sh), and interbedded fines and sand (Sh; Fl) and are flat-lying, with gradational to sharp contacts. Individual laminae likely represent deposition from flood events, and the rhythmic pulsing of sediment-laden water though the passages as discussed in Ford & Williams (2007) and Plotnick et al. (2009), as they were taken in

either upper level passages which were relatively dry (CS 104) or lower level passages that are not currently experiencing continuous water flow (CS 104 and CS 106). Changes in grain size in these laminae are probably the result of changing water flow velocities due to flood events.

Core CS 104 was taken in a topographic low within a passage, near a pool containing mud rich deposits. A particularly sharp contact within the sediment is observed in CS 104 at 120 mm (Figure 9). Grain size is considerably coarser below the contact and finer above, indicative of a particularly distinct decrease in water flow velocity. Since this core was taken from the upper level of the cave system, this decrease in depositional energy may be a result of less floodwater reaching this passage over time as the cave stream slowly erodes further downward.

CS 105 was taken in a lower level passage against a wall that appeared to be a cut bank aside the main channel in the middle of the passage (Figure 7). The core was taken immediately adjacent to the base of this wall in an area possibly subject to enhanced erosion during flood events, so sediment within this core shows sharp contacts between facies types which may result from repeated episodes of erosion (Figure 6). Since CS 105 shows more distinct laminations in comparison to the other cores, these sharp contacts may simply be evidence for more frequent abrupt changes in flow energy levels to create the distinct laminae. CS 105 also contains coarser-grained sediment in comparison to the other cores in this study consisting predominantly of sandy material (Figure 6). The presence of coarse-grained material interbedded with thin laminae of finer grained

material corresponds to it being taken from the main flow channel part of the passage, rather than on a bank where finer deposits are generally located.

5.2 Sediment Accumulation Rates

If the assumption is made that the sediment accumulation rate of 1 mm per year is relatively consistent through the top 20 cm of the core, extrapolation of this rate (Table 3) to a depth of 20 cm below surface gives a corresponding date of approximately 200 years before present (AD 2016). This corresponds to the early 1800's, the time period when settlers began arriving and altering the landscape in the Horse Cave area (Edwards & Edwards Gardiner, 1940**;** Chaney, 2017). A colour change occurs in cores CS 302 (medium brown below and red above; 20 cm: Figure 4), CS 106 (9 cm: Figure 10) and CS 102 (6 cm: Figure 8). This abrupt change in sediment colour possibly correlates to the point in time when settlers first arrived in the Horse Cave area. Increased activity on the landscape due to land clearing, early infrastructure construction and agriculture alters the natural sediment flow processes and increases terrigenous input into the subsurface (Hostettler et al., 1999; Ekdahl et al., 2004). This increased terrigenous input is reflected in the Hidden River Cave sediment record as a change in colour from red to medium brown, likely as a result of increased organic matter content from surficial input (United States Department of Agriculture, 2017). Based on the assumption the colour change is related to settlement in the valley, accumulation rates calculated from cores showing this colour change (CS 302, CS 106 and CS 102) range from 0.45 – 1 mm per year. The correlation of a distinct change in cored sediment colour dated by Pb-210 to around the

year 1800 and the timing of historical anthropogenic settlement strengthens the idea that there is a direct connection between surface processes and the subsurface sediment record.

5.3 Connecting Historic Events to Sediment Deposits Using Relative Metal Concentrations

The CS 302 core plot (Figure 11) exhibits relatively consistent levels of chromium, copper and nickel between 110 mm depth from the surface to approximately 40 mm. The overall trend in the total counts values for each of the metals in core CS 302 slowly increases moving up the core from approximately 40 mm from the top. Sediment at 40 mm depth below surface has a corresponding Pb-210 accumulation date of between 1982 and 1988 (Figure 11). The gradual increase in metal concentrations towards the top of the core is directly connected to the opening of the metal plating plant Ken Dec in 1970. The most reliable Pb-210 dates were obtained from the upper 100 mm of core CS 302 where there is an excess of Pb-210 (Figure 11). The prominent analytical features in this section are the chromium, nickel and copper peaks between approximately 15 – 18 mm. The Pb-210 dates indicate that sediments at this depth in the core were deposited between 1996 – 2000 (20 mm) and just after 2007 (10 mm; Figure 11). Historical data indicate that from 2004 – 2009, the metal plating company Ken Dec was illegally discharging untreated metal plating effluent (US EPA, 2017). Therefore, the large metal peaks in the core record correspond to the time period when Ken Dec waste was being directly discharged into the Hidden River Cave system between 2004 and 2009.

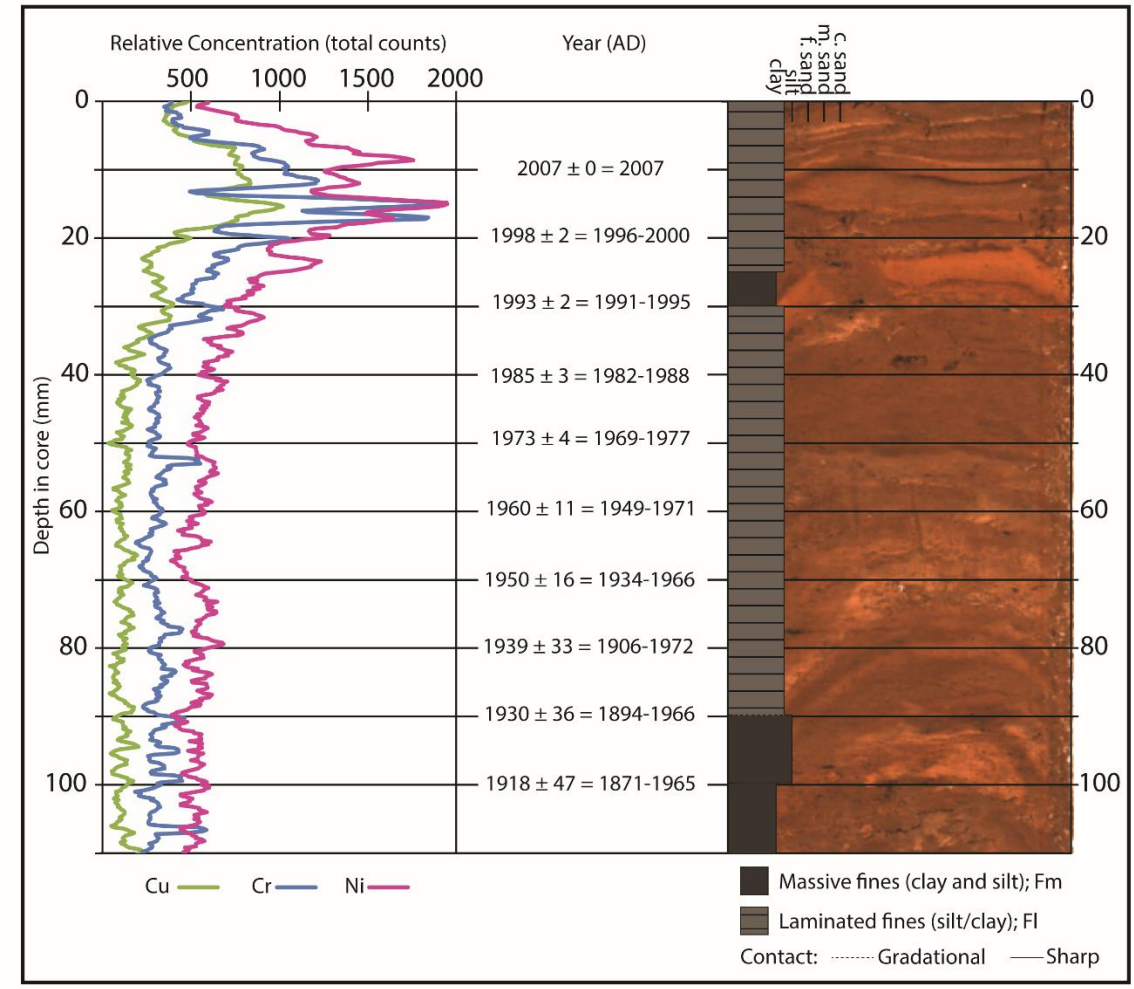

Figure 11: The upper section of core sample CS 302 showing Itrax elemental data on the left (see Fig. 4), lead-210 dates in the middle as years (AD), (with standard deviation values and the resulting year range) and the core image on the right overlain with a sedimentological log. Horizontal lines are drawn through the graph and core image corresponding with where lead-210 dates were analysed.

There appears to be a lag between the start-up of operations in 1970 and the appearance of increasing metal concentrations in the sediment record (Figure 11). This contrasts with more recent evidence for contaminant releases (EPA case, 2004-2009) where metal concentrations increase in the sediment concurrently with the contamination

(Figure 11). This is likely due to the mechanism of transport of effluent into the cave system in these two different scenarios. In the early years of Ken Dec operations, the plating effluent was passing through the sewage treatment plant (Lewis, 1993). As such, it took time for the metal waste to initially accumulate and show a signature in the sediment record above background levels. Gradual metal accumulation over the years is reflected as a progressive increase in the total counts values obtained for chromium, copper and nickel in the core. When the illegal dumping of untreated effluent directly into the ground occurred between 2004 and 2009 (US EPA, 2017), large spikes of metal total counts values are apparent in the sediment record (Figure 11).

5.4 Changes in Metal Concentrations Upstream to Downstream

Metal-laden effluent from Ken-Dec would have moved primarily through the South Branch (Figure 1) of the cave and past the CS 106, 104, 102, and 302 sampling sites (Figure 3), meaning a discussion of upstream to downstream differences in the core record should reflect decreasing concentrations of metals (Figure 12). The furthest upstream core sample (CS 106) is in closest proximity to the former location of Ken Dec (Figure 3). Situated below and slightly downstream of the metal plant, the core was initially expected to have the highest total counts values for chromium, nickel, and copper. However, sediments from CS 106 recorded the second-lowest total counts values for nickel and copper, and the lowest total counts values of chromium (Table 5; Figure 10, 12). Interestingly, CS 104, the core second most downstream of the plating plant had

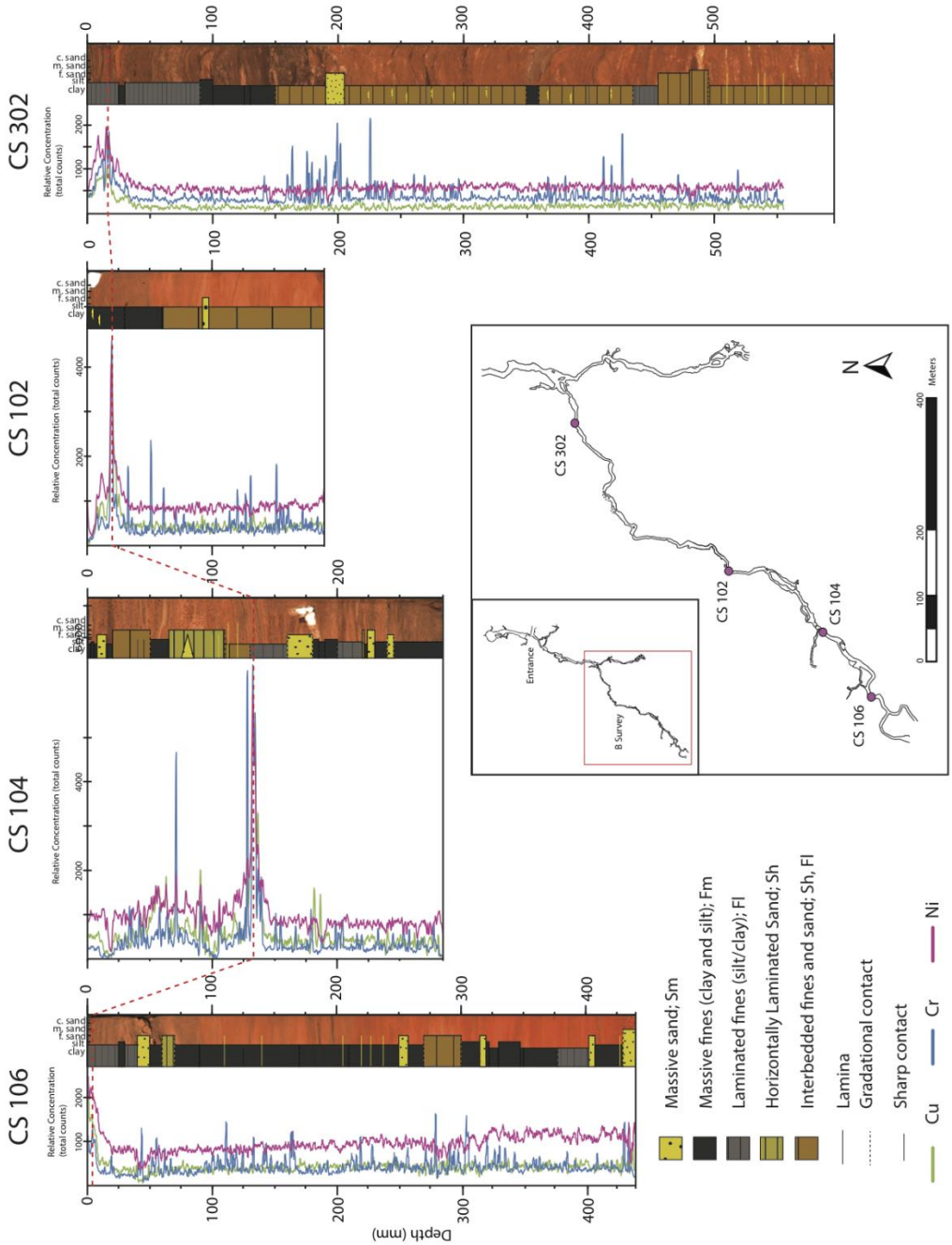

Figure 12: Correlation of relative metal concentrations in cores from the B-Survey Passage (CS 106, CS 104, CS 102, CS 302). Elemental data, sedimentological logs, and photographic images are shown for each core (see Figures 4, 8-10). Core locations are indicated on the inset Hidden River Cave passage map (see Figure 3). Cores are presented from the furthest upstream (left; CS 106) to furthest downstream (right; CS 302). The red dashed line correlates metal peaks (total counts) between cores which correspond to the illegal dumping of chrome plating waste between 2004-2009.

the highest total counts values for all three metals of interest (Table 5; Figure 9, 12). Karst systems contain varying levels of connectivity to the surface based on subsurface conduit development, and infiltration pathways are rarely linear and simple (Ford & Williams, 2007; Herman et al., 2012). As such, it is not illogical to suggest that the sinkhole where the illegal dumping occurred from 2004 – 2009 was more directly connected to the subsurface between the CS 106 and CS 104 sites. This would mean that most of the metal in the effluent from the dumping was deposited downstream of the CS 106 site but upstream of the CS 104 site and would explain the relatively low metal peak values in CS 106 and the highest recorded values in CS 104 (Figures 10, 9). Cores collected at sites further downstream from the metal plating plant show a progressive decrease in metal total counts values (Figure 12). CS 302, the core collected furthest downstream from the metal plating plant in this study, has the lowest total counts values for nickel and copper, and the second lowest for chromium (Figure 12). Since many contaminants, including chromium, nickel and copper, sorb onto sediment, metals would be deposited out of suspension with sediment (McLean & Bledsoe, 1992; Mahler et al., 1999; Bradl, 2004). As metal plating effluent moves downstream through the cave system with water and sediment, it would gradually reduce in concentration as it becomes diluted and deposited out of suspension. This trend is reflected in the total counts values for the sequence of cores examined in this study (Figure 12).

An alternative explanation for the apparent reduction in metal concentrations in sediment downstream of the plating plant relates to resuspension and reworking of initial contaminant deposits. Most sediment in a cave system is moved during high magnitude,

episodic flood events. It is therefore possible that sediment that was originally deposited at the CS 106 site (Figure 3) may have been initially deposited with higher metal concentrations and subsequently re-suspended in one or several flood events and redistributed downstream. This could also explain why CS 104 has the highest metal concentrations analysed (Figure 9). However, the CS 106 core was collected in a large cave room with relatively low ceilings (<5 feet high), a hummocky floor (hummocks <1 m high) and around 5-8 stagnant pools 1-3 m in diameter (Table 5; Figure 13). The pools are surrounded by rimstone dam formations which are sediment-free (Figure 14). There are no large sediment banks indicating waning flood flows, so it can be hypothesized that the area in which the rimstone dams have formed does not regularly experience large flood events. Therefore, it is unlikely that large amounts of flood-delivered contaminating metals would be present, or subsequently re-suspended and re-deposited downstream. It can therefore be confidently hypothesized that the connection between the sinkhole where the dumping of effluent waste from the metal plating plant occurred and the subsurface cave passage is somewhere between the core sites CS 106 and CS 104.

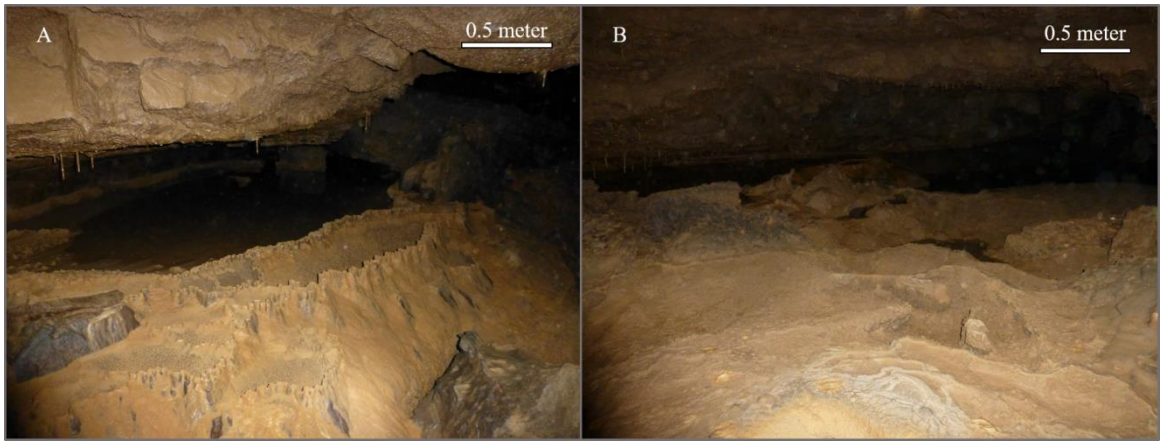

Figure 13: Photo showing the sampling location for core CS 106, a location in the cave system called the 'Rimstone Room'. This is a large cave room with ceilings <1.5 m high, a hummocky floor with hummocks <1 m high, and around 5-8 stagnant pools of water 1-3 m in diameter. A) stagnant pool surrounded by rimstone dams. B) Hummocky floor and stagnant pools. Blemishes on images are due to high moisture content in the cave air, and have been removed for photo clarity where possible. Photo by Russ Ellis.

Figure 14: Rimstone Dams. Example of rimstone dams found near sampling location of core CS 106. These indicate previous stagnant pools of water. Pencil in photo for scale. *Photo by Russ Ellis.*

Pb-210 dates confirmed that the large peaks between 15 – 18 mm in CS 302 are representative of the 2004-2009 illegal dumping from the former Ken Dec chrome plating plant. Cores CS 106, 104, and 102 also contain large, irregular peaks in relative metal concentrations in their core records (Figure 12). As such, it follows that these large metal peaks in CS 106, CS 104, and CS 102 core records can be correlated to the large peaks between 15-18 mm in CS 302, and that they also correspond to the Ken Dec illegal dumping (Figure 12). This distinct contamination event provides a stratigraphic marker that can be correlated across multiple cores along a passage in the cave system, also allowing for comparison of sediment accumulation rates within the cave system. Sediment accumulation rates can be calculated based on using the largest peak in the metal record (Table 5) and an average of 10 years time between the illegal dumping and core sampling. As a result, average accumulation rates range from 0.04 – 13.2 mm per year, reflecting the varied depositional environments within the cave system.

The entire analytical graph for core CS 302 (Figure 4**)** displays several chromium peaks (i.e. those clustered around 200 mm and 425 mm depth; Figure 4) in addition to the ones discussed above between 15-18 mm. However, the chromium peaks in the lower part of the core show very rapid changes in value and may represent natural chromium deposition in the sediment during single flood events.

5.5 Complexities of Sediment Transport and Deposition in Caves

Due to the complex nature of water movement in a cave system, sediment transport is complicated in nature. Varying depositional environments and passage sizes change how sediment and water move in various parts of the cave (Bosch & White, 2004; Ford & Williams, 2007). Certain areas like upper levels of the cave experience less sediment delivery than others, such as lower levels with continuously flowing water. Karst cave systems contain many different conduits and flow pathways that are inaccessible to humans but can host water and sediment flow. Sediment plumes may split in many different directions after entering the cave system, and it is difficult to ascertain whether the same sedimentation event reaches each of the depositional areas discussed in this study. Sediment accumulation rate almost certainly differs at different locations within the cave, and sedimentary fill does not form homogenously throughout the cave system (Arriolabengoa et al., 2015). This wide variety of conditions and potential flow paths makes it difficult to correlate specific beds or lamina between cores, even within the same passage. Broad trends such as the overall increase in chromium, copper and nickel concentrations are easier to discern.

6. Conclusion

This study explores the importance of understanding sediment dynamics in cave systems and the connection to transport and fate of contaminants in those systems. Sediment depositional patterns in the Hidden River Cave system are documented using

sediment core analysis. Facies types documented include massive sand (Sm), massive fines (clay and silt; Fm), laminated fines (clay and silt; Fl), interbedded fines and sand (Sh, Fl), and horizontally laminated sand (Sh).

One sediment core extracted from the Hidden River Cave system (Core CS 302, Figures 4, 11) was successfully dated using Pb-210 analysis and allows for the approximation of a sediment accumulation rates of 1 mm per year within the cave. Due the dynamic and varied environment in an active cave such as the Hidden River system, care must be taken while choosing the coring location, and subsequent samples from the sediment cores to be used for dating. Coring locations must be chosen based on knowledge of typical sediment deposition dynamics in a passage as well as assumed flood frequency within a particular passage. This was demonstrated with strategic coring locations in this study within a single passage (B Survey, Figure 3) and in areas with banks of sediment suitable for Pb-210 dating (CS 302, Figure 3, 4, 11).

Connections to surficial processes are apparent in the sediment record of the Hidden River Cave system. Historical chrome plating plant contamination events can be correlated to increases in relative metal concentrations in cored sediment using an ITRAX core scanner for determining elemental concentrations and Pb-210 dating techniques. Relative concentrations of metals accumulating in sediment tend to decrease downstream from the contamination source, indicating dilution of contaminants as deposition occurs moving downstream from the chrome plating plant. Lag time between contaminant input at the surface and deposition in the sediment record occurred when contaminants entered the cave system indirectly (i.e. after moving through the sewage treatment plant rather

than direct input). General trends in relative metal concentrations and sediment colour changes can be correlated between cores, but individual depositional events and laminae or beds are more difficult to correlate. Using the relative metal concentrations identified in a number of cores, especially CS 302, the effects of anthropogenic landscape development on sediment composition and chemistry can be determined and known contamination events are used as stratigraphic markers to correlate between cores in the same passage. Colour changes in the core, from medium brown to red downcore (Figures 4, 8, 10) appear to be the result of changing input into the cave system in the early 1800's at the same time as settlement was occurring in the Horse Cave area. This information is useful in understanding not only the paleo-record of anthropogenic activity on the surface, but also how that activity impacts the subsurface sediment and water. This helps to understand how best to protect the subsurface, especially when groundwater is used to support the communities living above.

With an enhanced suite of data including additional core analysis and chronological time constraint (i.e. Pb-210 dating), further understanding of subsurface processes and their relation to the surface can applied to further understand landscape evolution processes occurring within the basin of the cave system. Linking relative metal concentrations in the sediment deposit to specific historical events on the surface provides a basis for understanding past contamination events and how they moved through the cave system. This will inform how future contamination events may disperse through the system, using methodology that can be applied to other similar karstic systems. Further, this will inform public infrastructure, water and wastewater management planning so that

proper decisions can be made with respect to safety of communities overlying the cave system.

7. Future Work

As floodwaters rise, influx of surficial sediment or sediment reworking may cause peaks in metal concentrations to decrease downstream and be correlated across multiple cores. However, caves are hydrologically complex and flow is more complex than in surficial systems (Herman et al., 2012). As such, it is difficult to correlate individual beds or lamina across cores due to these complexities and varied/dynamic depositional environments. It is most logical to attempt to correlate between cores in the same passage, as is done across the B Survey (Figure 3) in this study with cores CS 106, 104, 102, and 302. Collection of additional cores from Hidden River Cave closer together and with even spacing throughout one passage would allow for a more detailed understanding of sediment accumulation patterns within the cave system. It would be ideal to fill in gaps in the B Survey passage, which has already shown elemental trends in chrome plating plant metals.

More general trends in metal or sediment characteristics are also an effective starting point for correlation between cores, to further understand how and by which pathways sediment moves through the cave system. This could be used in conjunction with tracer techniques such as dyes to gain valuable information in understanding the current sediment and water flow pathways (e.g. Herman et al., 2012). A noticeable

similarity between cores in this study is the distinct point of colour change from medium brown in the top sections of cores to red in the bottom sections. This colour change exhibited in CS 302 at 200 mm depth (Figure 4**)** is also reflected in cores CS 106 (Figure 10) and CS 102 (Figure 8) at 90 mm and 60 mm respectively. Based on historical data and Pb-210 dating, this colour change in CS 302 likely reflects increased terrigenous input to the subsurface as settlers began to arrive in the Horse Cave area and alter the landscape in the early 1800's. Further, it follows that the colour changes in cores CS 106 and CS 102 also reflect this point in time and can be correlated to the colour change in CS 302. Examination of a geochemical proxy such as elemental ratios of terrigenous source elements (Al, K, Ti, Zr) for terrigenous input (Zabel et al., 2001) and further Pb-210 dating in other cores from the Hidden River system would provide more evidence for this hypothesis, providing a strong research direction for the future. Caves are dynamic environments, and correlation between sediment deposits across the cave system is difficult but promising, based on the presented metal data, Pb-210 results and similar colour change patterns between the core records.

Other dating methods that have been used in cave studies are magnetostratigraphy, optically stimulated luminescence (OSL) and uranium-thorium dating of speleothems (Harmon et al., 1978; Zhang et al., 2010; Gazquez et al., 2014). These methods would further support the Pb-210 data presented in this study, and possibly provide additional data to further understand sediment transport and deposition in cave systems, and their connection to the surface.

Further studies in the Hidden River Cave system through analysis of additional cores and sediment tracing techniques will allow for a better understanding of sediment and contaminant transport and deposition in Hidden River Cave, and allow for application of this knowledge to other cave systems. The methodologies utilized for study of the Hidden River Cave system could be applied to various other cave systems to gain both a further understanding of sediment transport in cave systems and to add to the more generalized understanding of karstic landscape development.

8. References

American Cave Conservation Association (ACCA) (2013). Hidden River Cave & American Cave Museum: A Brief Introduction. Accessed on May 22, 2017 from http://hiddenrivercave.com/about.html.

Appleby, P.G., Oldfield, F., Thompson, R., Huttunen & Tolonen, K. (1979). 210Pb dating of annually laminated lake sediments from Finland. Nature, 280, p 53-55.

Appleby, P.G. & Oldfield, F. (1983). The assessment of 210Pb data from sites with varying sediment accumulation rates. Hydrobiologia, 103, p 29-35.

Blair, R.J., Ray, J.A., & O'dell, P.W. (2012). Integrated Surface Water and Groundwater Assessment of Large Springs in the Green River Basin (BMU4, Round 2). Report for the Kentucky Division of Water January 17, 2012.

Bosch, R.F., & White, W.B. (2004) Lithofacies and transport of clastic sediments in karstic aquifers, in Sasowsky, I.D., and Mylroie, J., Studies of Cave Sediments (Revised Edition ed.). Dordrecht: Springer, p 1–22.

Bradl, H. B. (2004). Adsorption of heavy metal ions on soils and soils constituents. Journal of Colloid and Interface Science, 277(1), p 1-18.

Bull, P.A. (1981). Some fine-grained sedimentation phenomena in caves. Earth Surface Processes and Landforms, 6, p. 11-22.

Carey, D.I. (2009). Green/Tradewater River Basin in Kentucky, Kentucky Geological Survey and University of Kentucky, map and chart 189, Series XII, 2009.

Cave Research Foundation (CRF) & West, David (2013). Hidden River Cave Survey Map and survey points data. Obtained from the Cave Research Foundation via David West. 4 map pages.

Chaney, C. (2016; 2017). Local Historian and Bookkeeper of the Town of Horse Cave, Kentucky. Personal Interview.

Collins, S.V., Reinhardt, E.G., Rissolo, D., Chatters, J.C., Nava Blank, A, & Luna Erreguerena, P. (2015). Reconstructing water level in Hoyo Negro, Quintana Roo, Mexico, implications for early Paleoamerican and faunal access. Quaternary Science Reviews, 124, p 68-83.

Dart Container Corporation (2017). "The Dart Story | US", accessed on April 25, 2016 from https://www.dartcontainer.com/about-us/dart-history/.

De Waele, J., Plan, L., & Audra, P. (2009). Recent developments in surface and subsurface karst geomorphology: An introduction. Geomorphology, 106, p 1-8.

Dogwiler, T., & Wicks, C., 2004, Sediment entrainment and transport in fluviokarst systems. Journal of Hydrology, 295, v. 1-4, p 163-172.

Edwards, C., & Edwards Gardiner, F. (1940). Cyrus Edwards' Stories of Early Days and Others in What Is Now Barren, Hart and Metcalfe Counties. Louisville, KY: Standard Print., 1940, p 94-114.

Ekdahl, E.J., Teranes, J.L., Guilderson, T.P., Turton, C.L., McAndrews, J.H., Wittkop, C.A. & Stoermer, E.F. (2004). Prehistorical record of cultural eutrophication from Crawford Lake, Canada. Geology, 32(9), p 745-748.

Farrant, A.R. & Smart, P.L. (2011). Role of sediment in speleogenesis; sedimentation and paragenesis. Geomorphology, 134, p 79-93.

Farrant, A. R., Smith, C. J., Noble, S. R., Simms, M. J., & Richards, D. A. (2014). Speleogenetic evidence from Olof Draenen for a pre-Devensian glaciation in the Brecon Beacons, South Wales, UK. Journal of Quaternary Science, 29(8), p 815-826.

Ford, D., and Williams, P. (2007). Karst Hydrogeology and Geomorphology. Chapters 5: Karst Hydrology, and Chapter 8: Cave Interior Deposits. Chichester: John Wiley & Sons, 2007. Print.

Foster, D. (2016). Director of the American Cave Museum, Horse Cave, Kentucky. Personal Interview.

Freeze, R.A, & Cherry, J.A. (1979). Chapter 2: Physical Properties and Principles in Groundwater. Upper Saddle River: Prentice Hall Inc. Print. p 14-79.

Gazquez, F., Calaforra, J.M., Forti, P., Stoll, H., Ghaleb, B., & Delgado-Huertas, A. (2014) Paleoflood events recorded by speleothems in caves: Earth Surface Processes and Landforms, 39, p 1345-1353.

Ghaleb, B. (2009). Overview of the method for the measurement and interpretation of short-lived radioisotopes and their limits. IOP conference series: Earth and environmental science., 5(1), IOP Publishing, p 1-13.

Gillieson, D. (1986). Cave sedimentation in the New Guinea Highlands. Earth Surface Processes and Landforms, 11, 533-543.

Google Earth (2017). Ruler measurement tool, Accessed online May 21, 2017.

Gregory, B.R.B., Peros, M., Reinhardt, E.G., & Donnelly J.P. (2015). Middle-late Holocene Caribbean aridity inferred from foraminifera and elemental data in sediment cores from two Cuban lagoons. Palaeogeography, Palaeoclimatology, Palaeoecology, 426, p 229-241.

Groves, C., & Meiman, J. (2005). Weathering, geomorphic work, and karst landscape evolution in the Cave City groundwater basin, Mammoth Cave, Kentucky. Geomorphology, 67, p 115-126.

Gulden, B. (2016). USA Longest Caves: NSS and Geo2 Long & Deep Caves Web Site, accessed May 22, 2017 from http://www.caverbob.com/usalong.htm.

Harmon, R. S., Thompson, P., Schwarcz, H. P., & Ford, D. C. (1978). Late Pleistocene paleoclimates of North America as inferred from stable isotope studies of speleothems. Quaternary Research, 9(1), p 54-70.

Hart County Chamber of Commerce (2014). Hart County Industry. Accessed online May 21, 2017 from http://www.hartcountyky.org/industry.html.

Health Canada (2017). Guidelines for Canadian Drinking Water Quality – Table 2: Chemical and Physical Parameters. Accessed May 7, 2017 from http://www.hc-sc.gc.ca/ewh-semt/pubs/water-eau/sum_guide-res_recom/index-eng.php#t2.

Herman, E.K., Toran, L., & White, W.B. (2012). Clastic sediment transport and storage in fluviokarst aquifers: an essential component of karst hydrogeology. Carbonates Evaporates, 27, p 211-241.

Hostettler, F.D., Pereira, W.E., Kvenvolden, K.A., van Geen, A., Luoma, S.N., Fuller, C.C. & Anima, R. (1999). A record of hydrocarbon input to San Francisco Bay as traced by biomarker profiles in surface sediment and sediment cores. Marine Chemistry, 64(1), p 115-127.

Hunsom, M., Pruksathorn, K., Damronglerd, S., Vergnes, H., & Duverneiul, P. (2005). Electrochemical treatment of heavy metals (Cu2+, Cr6+, Ni2+) from industrial effluent and modeling of copper reduction. Water Research, 39, p 610-616.

Jackson, B.P., Winger, P.V., & Lasier, P.J. (2004). Atmospheric Pb deposition to Okefenokee Swamp, Georgia, USA. Environmental Pollution 130. P 445-451.

Kambesis, P. (2007). The Importance of Cave Exploration to Scientific Research. Journal of Cave and Karst Studies, 69(1), p 46-58.

Karamanos, R.E., Bettany, J.R., & Rennie, D.A. (1976). Extractability of added lead in soils using lead-210. Canadian Journal of Soil Science. 56, p 37-42.

Kentucky Geological Survey (KGS) and The University of Kentucky (UKy) (2010). Karst Occurrence GIS polygon, based on Paylor & Currens, 2001, accessed on September 20, 2017 ("Karst geology—1:500,000") from http://www.uky.edu/KGS/gis/geology.htm.

Kentucky Geological Survey (KGS) and The University of Kentucky (UKy) (2012a). Strata of the Mississippian Age, accessed on May 21, 2017 from https://www.uky.edu/KGS/geoky/mississippian.htm.

Kentucky Geological Survey (KGS) and The University of Kentucky (UKy) (2012b). The Mississippian Plateau or Pennyroyal Region, accessed on May 21, 2017 from https://www.uky.edu/KGS/geoky/regionPennyroyal.html.

Lewis, J. (1993). Life Returns to Hidden River Cave: The Rebirth of a Destroyed Cave System. NSS News, July 1993, p 208-213.

Lintern, A., Leahy, P.J., Heijnis, H., Zawadzki., A Gadd, P., Jacobsen G., Deletic, A., & Mccarthy, D.T., (2016). Identifying heavy metal levels in historical flood water deposits using sediment cores. Water Research 105, p 34-46.

Loucks, R.G. (1999). Paleocave Carbonate Reservoirs: Origins, Burial-Depth Modifications, Spatial Complexity, and Reservoir Implications: AAPG Bulletin, 83(11), p 1795-1834.

Mahler, B.J., Lynch, L., & Bennett, P.C. (1999). Mobile sediment in an urbanizing karst aquifer: implications for contaminant transport. Environmental Geology, 39 (1), p 25-38.

Manufacturer's News Inc. (1997). 1998 Kentucky Manufacturer's Register. Evanston, IL, p 220-221.

McLean, J. E., & Bledsoe, B. E. (1992). Behavior of metals in soils. United States Environmental Protection Agency Ground Water Issue October 1992, p 1-25.

Miller, H., Croudace, I.W., Bull, J.M., Cotterill, C.J., Dix, J.K., & Taylor, R.N. (2015). Chapter 16 - Modern Pollution Signals in Sediments from Windermere, NW England, Determined by Micro-XRF and Lead Isotope Analysis, in Micro-XRF Studies of Sediment Cores: Springer Dordrecht, p. 423-442.

MyCore Scientific Inc (2017). www.mycore.ca.

National Oceanic and Atmospheric Administration (NOAA) (2017a). NOAA National Centers for Environmental information, Climate at a Glance: U.S. Time Series, Precipitation, published June 2017, retrieved on June 22, 2017 from http://www.ncdc.noaa.gov/cag/

National Oceanic and Atmospheric Administration (NOAA) (2017b). NOAA National Centers for Environmental information, Climate at a Glance: U.S. Time Series, Average Temperature, published June 2017, retrieved on June 22, 2017 from http://www.ncdc.noaa.gov/cag/

Newson, M.D. (1971). A Model of Subterranean Limestone Erosion in the British Isles Based on Hydrology. Transactions of the Institute of British Geographers, 54 (Nov), p 55-70.

Paylor, R.L., & Currens, J.C. (2001). "Karst Occurrence in Kentucky", Kentucky Geological Survey and University of Kentucky, map and chart 33, series XII, 2001.

Pflitsch, A., Wiles, M., Horrocks, R., Piasecki, J., & Ringeis, J. (2010). Dynamic Climatologic Processes of Barometric Cave Systems Using the Example of Jewel Cave and Wind Cave in South Dakota, USA. Acta Carsologica, 39 (3), p 449 – 462.

Plotnick, R., Kenig, F., Scott, A., Glasspool, I., Eble, C., & Lang, W. (2009). Pennsylvanian paleokarst and cave fills from northern Illinois, USA: A window into late Carboniferous environments and landscapes. PALAIOS, 24 (10), p 627-637.

Pohl, E.R. (1970). Upper Mississippian Deposits of South Central Kentucky – A Project Report. Transactions of the Kentucky Academy of Science, 31(1-2), P 1-15.

Ray, J.A., & Currens, J.C. September 1998. "Mapped Karst Ground-water Basins in the Campbellsville 30 x 60 Minute Quadrangle", Kentucky Natural Resources and Environmental Protection Cabinet – Division of Water and Kentucky Geological Survey, map and chart 17, series XI, 1998.

Reefnet Inc. (2006). Sensus Ultra Developer's Guide. Last Updated June 11, 2006, accessed July 25, 2016 from reefnet.ca/downloads.

Sasowsky, I.D., & Mylroie, J. (2007). Preface, in Sasowsky, I.D., and Mylroie, J., Studies of Cave Sediments: Physical and Chemical Records of Paleoclimate (Revised Edition ed.). Dordrecht: Springer, p v-viii.

Schroeder, J., & Ford, D. C. (1983). Clastic sediments in Castleguard Cave, Columbia Icefields, Alberta, Canada. Arctic and Alpine Research, p 451-461.

Shotyk, W., & Krachler, M. (2010). The isotopic evolution of atmospheric Pb in central Ontario since AD 1800, and its impacts on the soils, waters, and sediments of a forested watershed, Kawagama Lake. Geochimica et Cosmochimica Acta, 74, p 1963-1981.

Simon, A., Dickerson, W., & Heins, A. (2004). Suspended-sediment transport rates at the 1.5-year recurrence interval for ecoregions of the United States: transport conditions at the bankfull and effective discharge? Geomorphology, 58, p 243-262.

Springer, G.S., & Kite, J.S. (1997). River-derived slackwater sediments in caves along Cheat River, West Virginia. Geomorphology, 18, p 91-100.

Springer, G., Kite, J., & Schmidt, V. (1997). Cave sedimentation, genesis, and erosional history in the Cheat River Canyon, West Virginia. Geological Society of America Bulletin, 109(5), p 524-532.

Tenorio, J. A. S., & Espinosa, D. C. R. (2001). Treatment of chromium plating process effluents with ion exchange resins. Waste Management, 21(7), p 637-642.

The Horse Cave Heritage Festival (2002). A Leaf in Time: A pictoral history of Horse Cave, Kentucky, Vol 1. Compiled and published by The Horse Cave Heritage Festival, printed by Cave Country Print Shop.

The Kentucky Cabinet for Economic Development, Division of Research, in cooperation with Hart County Chamber of Commerce (1993). Resources for Economic Development: Hart County. Kentucky, p 10-11.

Thompson, P., Schwarcz, H. P., & Ford, D. C. (1976). Stable isotope geochemistry, geothermometry, and geochronology of speleothems from West Virginia. Geological Society of America Bulletin, 87(12), p 1730-1738.

United States Department of Agriculture (2017). Natural Resources Conservation Service: Soils. Accessed September 19, 2017 from https://www.nrcs.usda.gov/wps/portal/nrcs/detail/soils/edu/?cid=nrcs142p2_054286.

United States Department of the Interior: National Park Service (NPS). (2004). Mammoth Cave National Park Tract and Boundary Data. Accessed September 20, 2017 from https://catalog.data.gov/dataset/mammoth-cave-national-park-tract-and-boundary-data.

United States Department of the Interior: U.S. Geological Survey. (2014). Karst Topography - Teacher's Guide and Paper Model: USGS Geology in the Parks. Accessed from <http://geomaps.wr.usgs.gov/parks/cave/karst.html>.

United States Environmental Protection Agency (EPA) (2017). Summary of Criminal Prosecutions 2010, Case W.D. Kentucky 1:10CR-3-M. Accessed May 21, 2017 from https://cfpub.epa.gov/compliance/criminal_prosecution/index.cfm?action=3&prosecution_summary_id=2033.

U.S. Geological Survey (USGS) (2017). National Geospatial Program, 2016-11-03, USGS National Hydrography Dataset (NHD) Best ResolutionHU4-0511 2016--for HU-4 Subregion Shapefile Model Version 2.2.1: U.S. Geological Survey. Obtained from https://www.sciencebase.gov/catalog/item/581c247de4b09688d6e8852c.

Webb, R.S., & Webb, T. (1988). Rates of Sediment Accumulation in Pollen Cores from Small Lakes and Mires of Eastern North America. Quaternary Research, 30, p 284-297.

White, E.L., & White, W.B. (1968). Dynamics of Sediment Transport in Limestone Caves. National Speleological Society Bulletin, 30(4), p 115-129.

White, W., Watson, R., Pohl, E., & Brucker, R. (1970). The Central Kentucky Karst. Geographical Review, 60 (4), p 88-115.

White, W. B. (2007). Cave Sediments and Paleoclimate. Journal of Cave and Karst Studies, 69(1), p 76-93.

Zabel, M., Schneider, R.R., Wagner, T., Adegbie, A.T., de Vries, U., & Kolonic, S. (2001). Late Quaternary Climate Changes in Central Africa as Inferred from Terrigenous Input to the Niger Fan. Quaternary Research, 56, p 207-217.

Zhang, J., Huang, W., Yuan, B., Fu, R., & Zhou, L., (2010) Optically stimulated luminescence dating of cave deposits at the Xiaogushan prehistoric site, northeastern China. Journal of Human Evolution, 59(5), p 514-524.